An active atmospheric methane sink in high Arctic mineral cryosols

Supplementary Information

This supplementary file contains detailed methodology, supplemental figures (Fig. S1-S5) and tables (Table S1-S5), and additional references.

Methods and Materials

Field flux measurements

In situ CH_4 fluxes were measured in July 2011-2013 using a Picarro soil CO_2-CH_4 gas analyzer (Picarro Inc., Santa Clara, CA, USA) or Los Gatos Fast Methane Analyzer (Los Gatos Research Inc., Mountain View, CA) (Allan *et al.*, 2014; Stackhouse *et al.*, 2014 and this study).

Surface fluxes were measured in replicates using open-circuit dark chambers with continuous gas replacement from the air in 2011-2013 or closed-static chamber in 2013. For the open-circuit method, gas was continuously sampled (flow rate = 25 cm^3 min^{-1}) and analyzed at approximately 1 hz sample rate for CH_4, CO_2, H_2O, and $^{13}CO_2$, with alternating analysis periods of atmosphere and standard calibration gas. The flux chamber interior was continuously mixed with a small fan, and sample periods ranged from 45-600 min, with 45 min found to be the time needed to reach steady state concentration. The CH_4 uptake rates were calculated from the difference between initial atmospheric CH_4 concentration and the stabilized CH_4 concentration, with molar volume corrected for

temperature using soil surface temperature and barometric pressure. For the closed-static method, the net loss of CH_4 was calculated by comparing the initial atmospheric CH_4 concentration and the final CH_4 concentration being measured at the end of a 4-minute duration. Subsurface CH_4 concentration was measured directly using gas sipper tubes installed into shallow boreholes at various depths and sealed into place with bentonite clay to prevent atmospheric contamination. Soil temperatures at corresponding depths were measured by LiCOR thermistor (Maxim Integrated Products, San Jose, CA, USA).

Long-term intact core warming experiments

The setup of this warming experiments being described briefly here is paraphrased from a submitted manuscript, (Stackhouse *et al.*, 2014), to provide basic information that is essential for understanding the metagenome and metaproteome analyses performed in this study.

Seventeen 1-m long core samples, collected from a 16x16 m rectangular, ice-wedge polygon at the study site, were divided into four treatments: saturated (4 cores, mimicking thermokarst-affected terrain), *in situ* (7 cores, *in situ* soil water saturation conditions), dark (2 cores), and a control group (4 cores, remain frozen below 70 cm). Initially, core samples were kept frozen in insulated 55 gallon barrels that were filled with 20% ethanol bath maintained at -3°C by recirculating thermochillers (ThermoCube 200-LT, Solid State Cooling System, USA). The cores were individually wrapped in double layers of plastic trash bag to prevent direct contact with the ethanol bath. The

cores then underwent a progressively thawing, that took 13 weeks, to ~4°C in a walk-in cold room from top to bottom (except for the control group, which were thawed to 70 cm to keep the permafrost layer frozen), by adjusting the level of the ethanol bath.

Prior to thawing (T=0), small holes were drilled using a sterilized drill bit at 5 cm, 35 cm, 65 cm and ~80 cm (below permafrost table). From one replicate core of each treatment, frozen soil samples (10-15 g) were collected with a sterilized spatula at each depth for molecular analyses. After collection, the hole was plugged with a 1.3-cm diameter butyl-rubber stopper and sealed with waterproof tape. Similarly, cryosol samples were collected after 1-week thawing at each depth (T=0.25 month) from the same replicate cores processed at T=0. At later time points (T=6, 12 and 18 months post thaw), cryosol samples were collected from different replicate cores for each treatment in order to minimize unappreciated effect on the overall porosity of the cores due to soil removal.

During the long-term warming experiment, gas samples from the headspace of all 17 cores were analyzed for O_2, N_2, CO_2, CH_4, H_2 and CO. Rhizon tubes (2.5 mm diameter, 50 mm length) were installed at 5 cm, 35 cm, 65 cm and ~80 cm near the drill holes from which cryosol samples were collected. Pore water samples were collected using Rhizon tubes and were analyzed for aqueous chemistry. Operation details, results and discussion are presented in (Stackhouse *et al.*, 2014).

Abundance of methanotrophs and methanogens in metagenomic studies

As part of the long-term intact core warming experiments, 4 g of cryosols were collected and processed as described in (Stackhouse *et al.*, 2014). Total DNA was extracted using Fast DNA SPIN Kit (MP Biomedical, Irvine, CA) (Vishnivetskaya *et al.*, 2014). The extracted DNA samples were used to prepare metagenome shotgun libraries using the Illumina Nextera DNA library preparation kit (Illumina, Inc., San Diego, CA, USA), and sequenced (2 x 100 bp) on an Illumina HiSeq 2000 platform (Chauhan *et al.*, 2014). Results of 16 near-surface (at 5 cm depth) cryosoal samples representing different time point (T=1 week, 6 and 12 months) were analyzed.

Raw data was processed through MG-RAST pipeline (Meyer *et al.*, 2008) which first demultiplexed and removed sample identifier and then joined overlapping pair-end reads. Low quality sequences, artificial duplicate sequences were removed as part of the quality control (QC) pipeline. The number of post-QC reads per library averaged 1.7 x 10^7 with an average library size of 4.85 Gbp. All gene features were predicted and annotated by searching against M5NR database and taxonomically classified to species level by "Best Hit Classification" using the default values (Max. e-Value Cutoff=$1e^{-5}$, Min. % Identity Cutoff = 60% and Min. Alignment Length Cutoff = 15). The frequency data of these 16 libraries was exported from MG-RAST into STAMP for statistical analyses (Parks & Beiko, 2010). Hit abundance data was normalized to the total sequences passing the QC pipeline. Only the methanotrophic and methanogenic genera (as reviewed by (Nazaries *et al.*, 2013)) with relative abundances > 0.001% were considered. The relative abundance of individual genus was not statistically different at

alpha=0.05 (ANOVA in STAMP) and therefore means (and standard deviations) of all 16 samples were reported.

Assembly of pmo gene from metagenomes and their abundances

De novo co-assembly of raw sequences from 10 libraries (five 1-week and five 6-months thawed samples at 5 cm depth) were performed using MetaVelvet (Namiki *et al.*, 2012). Functional classifications were annotated separately via IMG/ER and MG-RAST (ID: 4530050.3) using SEED Subsystem and GenBank using the default values (Max. e-Value Cutoff=$1e^{-5}$, Min. % Identity Cutoff = 60% and Min. Alignment Length Cutoff = 15). Contigs identified as "methane monooxygenase" were searched for protein-coding genes because they may contain fragments of more than one gene. Phylogenetic affiliation of individual gene was queried against the NCBI non-redundant protein database using BlastX.

Raw reads were mapped to each of contigs, that are comprised of *pmo* genes (encodes for particulate methane monooxygenase), using Bowtie (Langmead *et al.*, 2009) to compute the relative abundance. Mean abundances (and standard deviations) of 16 samples were calculated by dividing the number of matched reads by the total number of mappable reads. Co-assembly of sequences from multiple libraries usually masks the genetic variations within and between populations or libraries, and the resultant contigs likely contain mixed genetic signals from the dominant population. We used prefix pan- to indicate that the detected genes are not derived from a single clonal population.

De novo assembly is more preferred when compared to reference-based assembly because the latter prevents the discovery of new genotypes variants by setting an *a priori* framework for read alignment. Nonetheless, raw reads of five 1-week thawed samples (5 cm depth) were mapped to the representative *pmoCAB* operon of USCα recovered by bacterial artificial chromosome (BAC) cloning (GenBank Acc. No. CT005232) (Ricke *et al.*, 2005) to demonstrate that a complete *pmoCAB* operon of the USCα genotype was successfully assembled from our data.

Phylogenetic analyses of pmo genes

Phylogenetic trees were constructed from deduced amino acid (aa) sequences for *pmo*A, *pmo*B and *pmo*C genes that encodes for α, β and γ subunit, respectively. All sequences had no frame-shift errors and no curation was applied. Three datasets were created. The *pmoA* gene dataset contained (1) aa sequences of pan-*pmoA* genes from this study. One of them was too short and thus omitted; (2) aa sequences of the best three BlastX matches; (3) aa sequences of all *pmoA* gene copies in published genomes of methanotrophs; (4) aa sequences of *pmoA* genes recovered from environmental studies of permafrost and atm CH_4-oxidizing sites; and (5) aa sequences of ammonia monooxygenases (*amoA* genes) that were used as the out-group. Sequences (2) – (5) were downloaded from NCBI (http://www.ncbi.nlm.nih.gov/). For cases where aa sequences were not available, nucleotide sequences were downloaded and translated. The dataset for *pmo*B and *pmoC* genes were created using the same approach.

For each dataset, sequences were aligned using MAFFT (Katoh *et al.*, 2005) included in freeware JalView package and manually edited using freeware Se-Al. Positions covered by more than half of the sequences were included while unaligned and ambiguous positions were trimmed. Alignments of 161 taxa and 171 aa (*pmo*A genes), 69 taxa and 377 aa (*pmo*B) genes) and 82 and 244 aa (*pmo*C genes) were used for phylogenetic tree construction. ProtTest (v3.3) (Darriba *et al.*, 2011) selected the best-fit amino acid evolutionary model (LG+G and LG+G for *pmo*A and *pmo*B and LG+I+G for *pmo*C gene) (Le & Gascuel, 2008) based on Bayesian Information Criterion. RAxML (v7.2.7 alpha) (Stamatakis, 2006; Stamatakis *et al.*, 2008) was used to search for the best-scoring maximum likelihood (ML) tree with the selected matrix and empirically estimated base frequencies, and to perform a rapid bootstrap analysis of 100 iterations in single run. Tree editing was done using freeware FigTree (v1.3.1).

Assembly of pmo genes from metatranscriptome and their abundances

Cryosols for metatranscriptomic analysis were collected on July 15, 2013 from an ice-wedge polygon, namely polygon interior and trough (79°24'57"N, 90°45'48"W). The samples were preserved using LifeGuard™ Soil Preservation Solution (MO BIO Laboratories Inc., Carlsbad, CA, USA) and stored at -20°C. Total RNA was extracted from 15 g of soil using the RNA PowerSoil Total RNA Isolation Kit (MO BIO Laboratories Inc., Carlsbad, CA, USA). Illumina TruSeq libraries were generated from the total RNA following manufacturer's protocols (Illumina) and sequenced on MiSeq (1 x 150 nt). After filtering and trimming using CLC Genomics Workbench (version 7.0)

(CLC bio, Boston, MA, USA), the number of reads obtained for the polygon interior and trough sample were 18,390,227 and 11,577,752 respectively. Then the post-QC reads were mapped to the USCα *pmoCAB* operon (GenBank Acc. No. CT005232) (Ricke *et al.*, 2005).

The reads were also assembled using CLC Genomics Workbench (built-in assembler velvet) and uploaded to MG-RAST for annotation (ID 4548476.3 and 4548477.3 for the polygon interior and trough sample respectively). Within CLC Genomics Workbench, metatranscriptomic reads were mapped against the metatransriptome (or transcript) contigs to determine read abundances (the number of matched reads divided by the total number of mappable reads). Transcript contigs were blasted against the assembled metagenome contigs from the 5 cm soil samples (ID 4530050.3) to determine the proportion of transcript contigs that are similar to the metagenome contigs. Transcript contigs containing *pmo*B genes were translated and used as template for the alignment of the peptide sequences detected from the proteome experiment (described below).

Identification of pMMO in metaproteome

Cores showing high CH_4 uptake flux in the intact core thawing experiment (Stackhouse *et al.*, 2014) were selected. Cryosols at 5 cm depth from 1-week drained cores were subsampled and kept frozen at -20°C. Three grams of cryosol was mixed with SDS-based lysis buffer and the slurry subjected to 15 min of boiling in a water bath with

intermittent vortexing as described earlier (Chourey *et al.*, 2010). The slurry was briefly cooled and centrifuged at 21,000 g for 15 min and supernatant aliquoted to fresh tubes and amended with chilled 100% TCA to final concentration of 25% followed by an overnight incubation at -20°C. The TCA-precipitated proteins were collected via centrifugation at 21,000 g for 15 min and the resulting protein pellet was washed with chilled acetone (thrice), air dried and solubilized in guanidine buffer [6M Guanidine HCl, 10 mM DTT in Tris $CaCl_2$ buffer (10 mM Tris, 50 mM $CaCl_2$, pH 7.8)] as described earlier (Chourey *et al.*, 2010). Total protein extracted from the samples was estimated using the RC/DC protein estimation kit (Bio-Rad Laboratories, Hercules, CA, USA) as per the manufacturer's protocol. The dissolved protein sample was subjected to trypsin proteolysis for 16 h at 37°C as described earlier (Chourey *et al.*, 2010; Brown *et al.*, 2006). The reaction was stopped by adding 10% formic acid to final concentration of 0.1% and kept frozen at -80°C until MS analysis.

An aliquot of digested peptides was pressure loaded onto an in-house packed SCX (Luna)-C18 (Aqua) column. The loaded sample column was subjected to an offline wash with solvent A (5% acetonitrile, 0.1% formic acid in HPLC-grade water) for 5 min followed by a gradient with 100% solvent B (70% acetonitrile, 0.1% formic acid in HPLC-grade water) over 10 min. This step was repeated 3 times for a total offline wash time of 45 min to desalt the column and get rid of any loosely attached contaminants. The sample column was then connected to an in-house C18 packed Picofrit column (New Objective, Woburn, MA) and the setup aligned on a Proxeon nanospray source in front of an LTQ-Orbitrap (Thermo Fisher Scientific Inc., San Jose, CA, USA) coupled to an

Ultimate 3000 HPLC system (Dionex^{TM}, Thermo Fisher Scientific, Waltham, MA, USA). Peptides were chromatographically separated and analyzed via 24 h Multi-Dimensional Protein Identification Technology (MuDPIT) approach as described earlier (Thompson *et al.*, 2006; Sharma *et al.*, 2012) and the tandem mass spectra (MS/MS scans) were acquired in a data dependent mode using Xcalibur software, V2.1.0 at settings described previously (VerBerkmoes *et al.*, 2009). The raw spectra acquired by 12-step MS/MS runs were searched via SEQUEST v.27 (Eng *et al.*, 1994) against an artificially constructed pMMO database using parameters described elsewhere (Thompson *et al.*, 2006; Sharma *et al.*, 2012). The output files were sorted and filtered using DTASelect v. 1.9 (Tabb *et al.*, 2002) with Xcorr values of at least 1.8 (+1), 2.5 (+2), 3.5 (+3). Identification of at least two peptides per protein sequence was set as criteria for positive protein identifications. Three technical replicates were analyzed for each protein sample.

pMMO database included amino acid sequences translated from (1) *pmo* contigs co-assembled from DNA sequences of the 10 metagenomic libraries stated above; (2) *pmo* contigs assembled from subsets of raw metagenome reads annotated as "methane monoxygenase" by MG-RAST and JGI/IMG; (3) *pmo* contigs generated by mapping to the USCα *pmoCAB* operon (GenBank Acc. No. CT005232) (Ricke *et al.*, 2005); and (4) *pmo* genes of methane monoxygenases obtained from GenBank. Sequences of common contaminants such as trypsin and keratin were also concatenated to the database.

Microcosm incubation experiments

Two sets of microcosms were set up to study the effect of water saturation and temperature on atm CH_4 oxidation rates. Prior to the experiment, 160 mL serum vials were soaked in 10% HNO_3 overnight to remove trace metals, rinsed using distilled water and combusted at 450°C for 8 h. New butyl rubber stoppers were boiled in 0.1 N NaOH for 45 min, soaked in distilled water for 8 hours and autoclaved.

A frozen core collected in April 2011 (Stackhouse *et al.*, 2014) was dissected into sections for every 10 cm. The peripheral rim of 5-cm thick was discarded to remove any potential contaminants from the core liner. The pristine cryosols were put into sterile Whirl-pak bags and homogenized by hand. The 0-10 cm section was used in this experiment. The original water content of the sample was determined to be 30.4±2.0 wt% by drying three subsamples of 5 g at 50°C for four days. The cryosols were visibly fully saturated, thus 10 wt%, 20 wt% and 30 wt% were regarded as equivalent to water saturation levels of 33%, 66% and 100% respectively. Cryosols were preconditioned to attain the desired water saturation by storing subsamples in a desiccator at 4°C. Eight to ten grams (wet weight) of cryosol were put into vials and sealed with treated butyl rubber stoppers and Al-crimps. Blank vials containing no soils were used to track abiotic gas exchanges and minor instrumental drift.

Manufactured air (Airgas USA LLC, PA, USA) was used to flush the headspace for 2-4 min. The gas composition of the manufactured air was analyzed by Peak Performer 1 gas chromatography systems (Peak Laboratories LLC, CA, USA), which are equipped with a thermal conductivity detector (for O_2 and N_2), a reduced compound

detector (for H_2 and CO) and a flame-ionization detector (for CO_2 and CH_4). Argon (ARUHP300, Airgas USA LLC, PA, USA) was used as carrier gas at a pressure of 82 psi. Calibration curves for O_2 and N_2 were generated from dilutions of fresh outdoor air in Argon. Standard gas (Scotty® Analyzed Gases, Air Liquide America Specialty Gases LLC, PA, USA) containing 1% atm of CO, CO_2, H_2, CH_4 and C_2H_4 was diluted in Argon to make gas mixtures of 0.5, 1, 2.5, 5, 7.5 and 10 ppm for all gases and 50, 100, 500 and 1000 ppm for all gases except H_2 and CO. Three measurements were made for each dilution. All calibration curves have high correlation coefficient ($R^2 > 0.99$).

Additional manufactured air was injected with a gas-tight glass syringe to over-pressurize the vials to 1.5 atm. All treatments were run in triplicates. One set of 12 vials was incubated at 4°C while another set was incubated at 10°C. Gas was sampled from the headspace at T=0, twice for the first 2 weeks and weekly for another 2 weeks (period of incubation = 31 days). Headspace volume was maintained by replacement of respective gas. Analysis was performed on Picarro iCO2 (Model # G2101-I) using the G2101-i coordinator (Picarro Inc., Santa Clara, CA, USA). Instrumental sample dilution was accounted for by multiplying a factor of 1.302 and the values were then corrected for dilution due to replacement.

The conversion between moles and ppm followed the ideal gas law:

$$10^{-6} mol = ppmv \times \frac{V}{RT}$$ Eq. 1

where V is volume in L; R is gas constant, 0.0821 Latm $K^{-1}mol^{-1}$; T is temperature in K

Atm CH_4 oxidation follows first-order kinetics and hence rate constants, *k*, were calculated and used to estimate the oxidation rates at standardized CH_4 concentration of 1.813 ppmv and expressed in nmol (g of soil)$^{-1}$ day^{-1}.

Atm CH_4 oxidation rates obtained from microcosms experiments were scaled up to CH_4 fluxes to compare with the *in situ* flux measurements at the field. The following formula was used:

$$F = \frac{r \times FW}{d \times D}$$

where *F* is CH_4 flux in mg C m^{-2}day^{-1}; *r* is CH_4 oxidation rate in nmol g^{-1}day^{-1}; *FW* is formula weight of carbon, 12 g; *d* is density; *D* is depth in m

Eq. 2

The density of 1.8x10^6 g m^{-3} (Stackhouse *et al.*, 2014) was used and the assumption of methanotrophic activity within the first 5 cm of active layer was taken. This may underestimate the flux values because field flux measurements indicated that atm CH_4 oxidation at AHI occurred down to 45 cm depth.

Temperature coefficients (Q_{10})

Q_{10} is used to measure the rate of change of a chemical or biological reaction as a consequent of temperate increase of 10°C. It is a factor calculated from the following equation:

$$Q_{10} = \left(\frac{R_2}{R_1}\right)^{\left(\frac{10}{T_2 - T_1}\right)}$$

where R_2 and R_1 are rates, in the same unit, measured respectively at T_2 and T_1, in the same unit; for $T_2 > T_1$

Eq. 3

Q_{10} values were computed for methanotrophy using (1) mean CH_4 oxidation rates obtained from microcosms for each treatment and corresponding incubation temperatures; and (2) mean CH_4 oxidation rates reported in the literature for which

temperature data was available. The criterion that the temperature difference between T_2 and T_1 being larger than 5°C was applied.

Arrhenius relationship between in situ CH_4 uptake flux and surface soil temperature

Since we are cautious about quantitatively extrapolating the observed effects of temperature and water saturation under laboratory conditions to the real situation and model prediction, only CH_4 fluxes and the corresponding surface soil temperatures measured during 2011-2013 expeditions were used to determine the Arrhenius relationship. Fluxes measured by open-circuit chambers were used to determine the relationship whereas those measured by closed-static chambers were excluded to eliminate the variation resulted from different collection methods (Whalen *et al.*, 1992). Natural logarithm of CH_4 uptake fluxes (y-axis) was plotted against 1000/temperature (x-axis) to create an Arrhenius plot, which showed a potential change in the slope. The data was then analyzed using the "Segmented" R package (cran.r-project.org/web/packages/segmented/). Davies' test was used to determine whether the change in the slope was statistically significant. Given the result suggested a breakpoint occurred at 3.588 (equivalent to 5.6°C; p = 0.006), function *segmented()* was used to estimate the breakpoint and the slopes (Results in Fig. S7).

Linear regression equations were fitted to data points below and above 5.6°C.

$$LN(F) = \frac{-Ea}{R}(\frac{1000}{T}) + LN(A) \quad \text{Eq. 4}$$

where F is CH_4 flux in mg C $m^{-2}day^{-1}$; E_a is activation energy in kJ mol^{-1}; R is gas constant, 8.314 J $K^{-1}mol^{-1}$; T is temperature, in K; density; A is pre-exponential factor

Q_{10} and active energy (E_a) of atm CH_4 oxidation were derived from Eq. 3 and Eq. 4 respectively. 95% confidence intervals were calculated for each slope.

For comparative purpose, other data were overlain on the plot (Fig. 4), which include: (1) CH_4 fluxes estimated from our microcosm experiments at 2.0 ppmv of CH_4; (2) CH_4 fluxes estimated from intact core thawing experiments (Stackhouse *et al.*, 2014); and (3) atm CH_4 oxidation sites at lower latitudes.

Estimation of monthly and annual atm CH_4 uptake fluxes

Monthly air temperatures at AHI during 1990s and 2090s were simulated through the Climate Model Intercomparison Project (CMIP5) using 8 climate models (BCC-CSM1.1, CCSM4, CSIRO-Mk3.6.0, GFDL-ESM2M, GISS-E2-R, HadGEM2-AO, IPSL-CM5A-MR and NorESM1-M) (Taylor *et al.*, 2012). The 'high emissions scenario' assuming mitigation policies in action (RCP8.5) was used to project the climate change in 2090s. Monthly and annual atm CH_4 uptake were estimated for temperatures from each model with the following assumptions:

a) Atm CH_4 uptake occurs at ground temperatures above 0°C. Field measurements taken during initial thaw in 2013 when soil surface temperature slowly warmed from -2°C to 10°C, CH_4 uptake increased from undetectable to -0.24 mg CH_4-C m^{-2} day^{-1}). First detectable consumptive flux corresponded roughly to the time when soil surface temperature was consistently above freezing.

b) Atm CH_4 uptake fluxes increase with temperature following an Arrhenius relationship (Eq. 4) and at a faster rate below 5.6°C than that above 5.6°C.

The sum of monthly uptake fluxes multiplied by the number of days in the month equaled the mean annual uptake flux. Upper and lower 95% confidence intervals were regarded as maximum and minimum annual uptake fluxes. Multi-model means were obtained by taking average across all models.

Air temperatures at Eureka, Ellesmere Island, Nunavut, Canada (N80°00'03", W86°00'25"; 112 km NE of AHI) were available for 2010 and 2011 through Total Carbon Column Observing Network (TCCON) (Wunch *et al.*, 2011). Temperature data (T) from late March to August 2011 was used. Missing data was gap-filled by linear interpolation between the two neighboring values. The data of 2010 tracked nicely that of 2011, thus the average temperature in Sept 2010 was used to substitute the missing data of Sept 2011. Mean daily temperatures were calculated by averaging multiple measurements on the day, which were then averaged to give monthly temperatures. The monthly and annual uptake fluxes were estimated as aforementioned. Eureka is located at higher latitude where the temperature is slightly cooler than that at AHI. CH_4 uptake fluxes therefore were also calculated for T+1°C and T+6°C which, respectively, are more representative for our study site and also to mimic severe summer warming which was not projected by climate models.

Legends to supplementary figures and tables

Fig. S1. Phylogenetic tree of *pmo*A genes constructed from deduced amino acid sequences (161 taxa and 171 aa). Highlighted is the pan-*pmo*A gene recovered in this study. Sequences of ammonia-oxidizing monoxygenase (*amo*A) were used as the out-group. Clusters of atmospheric CH_4 oxidizers are annotated in reference to Kolb (2009) (Kolb, 2009). Bootstrap values greater than 50% are shown as branch label. The scale bar represents a substitution rate of 0.2 changes per position.

Fig. S2. Phylogenetic tree of *pmo*B genes constructed from deduced amino acid sequences (69 taxa and 377 aa). Highlighted are the pan-*pmo*B genes recovered in this study. Sequences of ammonia-oxidizing monoxygenase (*amo*B) were used as the out-group. Bootstrap values greater than 50% are shown as branch label. The scale bar represents a substitution rate of 0.2 changes per position.

Fig. S3. Phylogenetic tree of *pmoC* genes constructed from deduced amino acid sequences (82 taxa and 244 aa). Highlighted are the pan-*pmo*C genes recovered in this study. Sequences of ammonia-oxidizing monoxygenase (*amo*C) were used as the out-group. Bootstrap values greater than 50% are shown as branch label. The scale bar represents a substitution rate of 0.2 changes per position.

Fig. S4. Alignment of translated amino acids of *pmo*B contigs from metagenomic and metatranscriptomic libraries. Histidine residues (H33, H137 and H139) that coordinate the di-copper center (aka the active site of pMMO) are highlighted in blue. GenBank

sequences YP_115247 and CAJ01562 encode for pmoB of MOB *Methylococcus capsulatus* str. Bath and atmMOB USCα.

Fig. S5. Predicted monthly air temperatures at Axel Heiberg Island, Canada. Monthly air temperatures at AHI during 1990s and 2090s were simulated through the Climate Model Intercomparison Project (CMIP5). T: Gap-filled monthly air temperatures in 2011 at Eureka, Ellesmere Island, Nunavut, Canada downloaded from Total Carbon Column Observing Network (TCCON).

Table S1. CH_4 field fluxes in the Northern Circumpolar permafrost region.

Table S2. Methanotrophic (A) and methanogenic (B) taxa identified in near-surface cryosols (at 5 cm depth) in the intact core warming experiments.

Table S3. Genes of methane monooxygenases and homologous enzymes identified in (a) metagenome data from near-surface cryosols (at 5 cm depth) in the intact core warming experiments and (b) metatranscriptome data from the polygon trough sample (collected on July 15, 2013).

Table S4. Aerobic methanotrophs detected in Arctic permafrost-affected region.

Table S5. Methanotrophic proteins identified in near-surface cryosols (at 5 cm depth) in the intact core warming experiments.

References:

Adachi M, Ohtsuka T, Nakatsubo T, Koizumi H. (2006). The methane flux along topographical gradients on a glacier foreland in the High Arctic, Ny-Ålesund, Svalbard. *Polar Biosci* **20**:131–139.

Allan J, Ronholm J, Mykytczuk NCS, Greer CW, Onstott TC, Whyte LG. (2014). Methanogen community composition and rates of methane production in Canadian high Arctic permafrost soils. *Environ Microbiol Rep* **6**:136–144.

Bäckstrand K, Crill PM, Jackowicz-Korczyñski M, Mastepanov M, Christensen TR, Bastviken D. (2010). Annual carbon gas budget for a subarctic peatland, Northern Sweden. *Biogeosciences* **7**:95–108.

Barbier BA, Dziduch I, Liebner S, Ganzert L, Lantuit H, Pollard W, *et al.* (2012). Methane-cycling communities in a permafrost-affected soil on Herschel Island, Western Canadian Arctic: active layer profiling of mcrA and pmoA genes. *FEMS Microb Ecol* **82**:287–302.

Bockheim JG. (2007). Importance of cryoturbation in redistributing organic carbon in permafrost-affected soils. *Soil Sci Soc Am J* **71**:1335–1342.

Brown SD, Thompson MR, Verberkmoes NC, Chourey K, Shah M, Zhou JZ, *et al.* (2006). Molecular dynamics of the Shewanella oneidensis response to chromate stress. *Mol Cell Proteomics* **5**:1054–1071.

Brummell ME, Farrell RE, Hardy SP, Siciliano SD. (2014). Greenhouse gas production and consumption in High Arctic deserts. *Soil Biol Biochem* **68**:158–165.

Brummell ME, Farrell RE, Siciliano SD. (2012). Greenhouse gas soil production and surface fluxes at a high arctic polar oasis. *Soil Biol Biochem* **52**:1–12.

Chauhan A, Layton AC, Vishnivetskaya TA, Williams D, Pfiffner SM, Rekepalli B, *et al.* (2014). Metagenomes from thawing low-soil-organic-carbon mineral cryosols and permafrost of the Canadian high Arctic. *Genome Announc* **2**:e01217–14.

Chourey K, Jansson JK, VerBerkmoes N, Shah M, Chavarria KL, Tom LM, *et al.* (2010). Direct cellular lysis/protein extraction protocol for soil metaproteomics. *J Proteome Res* **9**:6615–6622.

Christensen TR, Friborg T, Sommerkorn M, Kaplan J, Illeris L, Soegaard H, *et al.* (2000). Trace gas exchange in a high-arctic valley 1. Variations in CO_2 and CH_4 flux between tundra vegetation types. *Glob Biogeochemcial Cycles* **14**:701–713.

Christiansen CT, Svendsen SH, Schmidt NM, Michelsen A. (2012). High arctic heath soil respiration and biogeochemical dynamics during summer and autumn freeze-in - effects of long-term enhanced water and nutrient supply. *Glob Chang Biol* **18**:3224–3236.

Darriba D, Taboada GL, Doallo R, Posada D. (2011). ProtTest 3: fast selection of best-fit models of protein evolution. *Bioinformatics* **27**:1164–1165.

Elberling B, Jakobsen BH, Berg P, Søndergaard J, Sigsgaard C. (2004). Influence of vegetation, temperature, and water content on soil carbon distribution and mineralization in four high Arctic soils. *Arctic* **36**:528–538.

Emmerton CA, St. Louis VL, Lehnherr I, Humphreys ER, Rydz E, Kosolofski HR. (2014). The net exchange of methane with high Arctic landscapes during the summer growing season. *Biogeosciences Discuss* **11**:1673–1706.

Eng JK, McCormack AL, Yates JRI. (1994). An approach to correlate tandem mass spectral data of peptides with amino acid sequences in a protein database. *J Am Soc MassSpectrometry* **5**:976–989.

Graef C, Hestnes AG, Svenning MM, Frenzel P. (2011). The active methanotrophic community in a wetland from the High Arctic. *Environ Microbiol Rep* **3**:466–472.

Johansen KML, Berg LK, Feld T. (2011). Methane fluxes measured at Flakkerhuk, Disko Island (West Greenland) at different vegetation specific sites. In: *Methane dynamics in a permafrost landscape at Disko Island, West Greenland (Field Course in Physical Geography 2011)*, Hansen, BU & Elberling, B (eds), Faculty of Science, University of Copenhagen, pp. 43–55.

Kaliuzhnaia MG, Makutina VA, Rusakova TG, Nikitin D V, Khmelenina VN, Dmitriev V V, *et al.* (2002). Methanotrophic communities in the soils of Russian northern taiga and subarctic tundra. *Mikrobiologiya* **71**:264–271.

Katoh K, Kuma K, Toh H, Miyata T. (2005). MAFFT version 5: Improvement in accuracy of multiple sequence alignment. *Nucleic Acids Res* **33**:511–518.

Kolb S. (2009). The quest for atmospheric methane oxidizers in forest soils. *Environ Microbiol Rep* **1**:336–346.

Kutzbach L, Wagner D, Pfeiffer E. (2004). Effect of microrelief and vegetation on methane emission from wet polygonal tundra, Lena Delta, Northern Siberia. *Biogeochemistry* **69**:341–362.

Langmead B, Trapnell C, Pop M, Salzberg SL. (2009). Ultrafast and memory-efficient alignment of short DNA sequences to the human genome. *Genome Biol* **10**:R25.

Le SQ, Gascuel O. (2008). An improved general amino acid replacement matrix. *Mol Biol Evol* **25**:1307–1320.

Liebner S, Rublack K, Stuehrmann T, Wagner D. (2009). Diversity of aerobic methanotrophic bacteria in a permafrost active layer soil of the Lena Delta, Siberia. *Microb Ecol* **57**:25–35.

Liebner S, Svenning MM. (2013). Environmental transcription of mmoX by methane-oxidizing Proteobacteria in a sub-Arctic palsa peatland. *Appl Environ Microbiol* **79**:701–706.

Liebner S, Wagner D. (2007). Abundance, distribution and potential activity of methane oxidizing bacteria in permafrost soils from the Lena Delta, Siberia. *Environ Microbiol* **9**:107–117.

Liebner S, Zeyer J, Wagner D, Schubert C, Pfeiffer E-M, Knoblauch C. (2011). Methane oxidation associated with submerged brown mosses reduces methane emissions from Siberian polygonal tundra. *J Ecol* **99**:914–922.

Lupascu M, Wadham JL, Hornibrook ERC, Pancost RD. (2012). Temperature sensitivity of methane production in the permafrost active layer at Stordalen, Sweden: a comparison with non-permafrost Northern Wetlands. *Arctic, Antarct Alp Res* **44**:469–482.

Mackelprang R, P.Waldrop M, DeAngelis KM, David MM, Chavarria KL, Blazewicz SJ, *et al.* (2011). Metagenomic analysis of a permafrost microbial community reveals a rapid response to thaw. *Nature* **480**:368–371.

Martineau C, Pan Y, Bodrossy L, Yergeau E, Whyte LG, Greer CW. (2014). Atmospheric methane oxidizers are present and active in Canadian high Arctic soils. *FEMS Microbiol Ecol* **89**: 257–269.

Martineau C, Whyte LG, Greer CW. (2010). Stable isotope probing analysis of the diversity and activity of methanotrophic bacteria in soils from the Canadian high Arctic. *Appl Environ Microbiol* **76**:5773–5784.

Mastepanov M, Sigsgaard C, Dlugokencky EJ, Houweling S, Ström L, Tamstorf MP, *et al.* (2008). Large tundra methane burst during onset of freezing. *Nature* **456**:628–631.

Meyer F, Paarmann D, M DS, Olson R, Glass EM, Kubal M. (2008). The metagenomics RAST server - a public resource for the automatic phylogenetic and functional analysis of metagenomes. *BMC Bioinformatics* **9**:386.

Namiki T, Hachiya T, Tanaka H, Sakakibara Y. (2012). MetaVelvet: an extension of Velvet assembler to de novo metagenome assembly from short sequence reads. *Nucleic Acids Res* **40**:e155.

Nazaries L, Murrell JC, Millard P, Baggs L, Singh BK. (2013). Methane, microbes and models: fundamental understanding of the soil methane cycle for future predictions. *Environ Microbiol* **15**:2395–2417.

Pacheco-Oliver M, McDonald IR, Groleau D, Murrell JC, Miguez CB. (2002). Detection of methanotrophs with highly divergent pmoA genes from Arctic soils. *FEMS Microbiol Lett* **209**:313–319.

Parks DH, Beiko RG. (2010). Identifying biologically relevant differences between metagenomic communities. *Bioinformatics* **26**:715–721.

Pickett-Heaps CA, Jacob DJ, Wecht KJ, Kort EA, Wofsy SC, Diskin GS, *et al.* (2011). Magnitude and seasonality of wetland methane emissions from the Hudson Bay Lowlands (Canada). *Atmos Chem Phys* **11**:3773–3779.

Ricke P, Kube M, Nakagawa S, Erkel C, Reinhardt R, Liesack W. (2005). First genome data from uncultured Upland Soil Cluster alpha methanotrophs provide further evidence for a close phylogenetic relationship to *Methylocapsa acidiphila* B2 and for high-affinity methanotrophy involving particulate methane monooxygenase. *Appl Environ Microbiol* **71**:7472–7482.

Sachs T, Wille C, Boike J, Kutzbach L. (2008). Environmental controls on ecosystem-scale CH4 emission from polygonal tundra in the Lena River Delta, Siberia. *J Geophys Res* **113**:G00A03.

Sharma R, Dill BD, Chourey K, Shah M, VerBerkmoes NC, Hettich RL. (2012). Coupling a detergent lysis/cleanup methodology with intact protein fractionation for enhanced proteome characterization. *J Proteome Res* **11**:6008–6018.

Stackhouse B, Vishnivetskaya T, Layton A, Pfiffner S, Mykytczuk N, Whyte LG, *et al.* (2014). Simulated spring thaw of permafrost from mineral cryosol reveals increaes in CO_2 emissions and atmospheric CH_4 sink. *J Geophys Res: Biogeo* **submitted**.

Stamatakis A. (2006). RAxML-VI-HPC: maximum likelihood-based phylogenetic analyses with thousands of taxa and mixed models. *Bioinformatics* **22**:2688–2690.

Stamatakis A, Hoover P, Rougemont J. (2008). A rapid bootstrap algorithm for the RAxML web servers. *Syst Biol* **57**:758–771.

Ström L, Tagesson T, Mastepanov M, Christensen TR. (2012). Presence of Eriophorum scheuchzeri enhances substrate availability and methane emission in an Arctic wetland. *Soil Biol Biochem* **45**:61–70.

Sturtevant CS, Oechel WC. (2013). Spatial variation in landscape-level CO2 and CH4 fluxes from arctic coastal tundra: influence from vegetation, wetness, and the thaw lake cycle. *Glob Chang Biol* **19**:2853–2866.

Sturtevant CS, Oechel WC, Zona D, Kim Y, Emerson CE. (2012). Soil moisture control over autumn season methane flux, Arctic Coastal Plain of Alaska. *Biogeosciences* **9**:1423–1440.

Tabb DL, McDonald WH, Yates JRI. (2002). DTASelect and contrast: Tools for assembling and comparing protein identifications from shotgun proteomics. *J Proteome Res* **1**:21–26.

Tagesson T, Mölder M, Mastepanov M, Sigsgaard C, Tamstorf MP, Lund M, *et al.* (2012). Land-atmosphere exchange of methane from soil thawing to soil freezing in a high-Arctic wet tundra ecosystem. *Glob Chang Biol* **18**:1928–1940.

Taylor KE, Stouffer RJ, Meehl GA. (2012). An overview of CMIP5 and the experiment design. *Bull Am Meteorol Soc* **93**:485–498.

Thompson MR, VerBerkmoes NC, Chourey K, Shah M. (2006). Dosage-dependent proteome response of Shewanella oneidensis MR-1 to acute chromate challenge. *J Proteome Res* **6**:1745–1757.

Tveit A, Schwacke R, Svenning MM, Urich T. (2012). Organic carbon transformations in high-Arctic peat soils: key functions and microorganisms. *ISME J* **7**:1–13.

VerBerkmoes NC, Russell AL, Shah M, Godzik A, Rosenquist M, Halfvarson J, *et al.* (2009). Shotgun metaproteomics of the human distal gut microbiota. *ISME J* **3**:179–189.

Vishnivetskaya T, Layton A, Lau M, Chauhan A, Meyers A, Murphy J, *et al.* (2014). Commercial DNA extraction kits impact observed microbial community composition in permafrost samples. *FEMS Microb Ecol* **87**:217–230.

Wagner D, Lipski A, Embacher A, Gattinger A. (2005). Methane fluxes in permafrost habitats of the Lena Delta: effects of microbial community structure and organic matter quality. *Environ Microbiol* **7**:1582–1592.

Wartiainen I, Hestnes AG, Svenning MM. (2003). Methanotrophic diversity in high arctic wetlands on the islands of Svalbard (Norway) — denaturing gradient gel

electrophoresis analysis of soil DNA and enrichment cultures. *Can J Microbiol* **612**:602–612.

Whalen SC, Reeburgh WS. (1990). Consumption of atmospheric methane by tundra soils. *Nature* **346**:160–162.

Whalen SC, Reeburgh WS, Barber VA. (1992). Oxidation of methane in boreal forest soils: a comparison of seven measures. *Biogeochemistry* **16**:181–211.

Wilhelm RC, Niederberger TD, Greer C, Whyte LG. (2011). Microbial diversity of active layer and permafrost in an acidic wetland from the Canadian High Arctic. *Can J Microbiol* **57**:303–315.

Wunch D, Toon GC, Blavier J-FL, Washenfelder RA, Notholt J, Connor BJ, *et al.* (2011). The Total Carbon Column Observing Network. *Phil Trans R Soc A* **369**:doi:10.1098/rsta.2010.0240.

Yergeau E, Hogues H, Whyte LG, Greer CW. (2010). The functional potential of high Arctic permafrost revealed by metagenomic sequencing, qPCR and microarray analyses. *ISME J* **4**:1206–1214.

Fig. S1 Phylogenetic tree of pmoA genes constructed from deduced amino acid sequences (161 taxa and 171 aa). Highlighted is the pan-pmoA gene recovered in this study. Sequences of ammonia-oxidizing monoxygenase (amoA) were used as the out-group. Clusters of atmospheric CH4 oxidizers are annotated in reference to Kolb (2009) (96). Bootstrap values greater than 50% are shown as branch label. The scale bar represents a substitution rate of 0.2 changes per position.

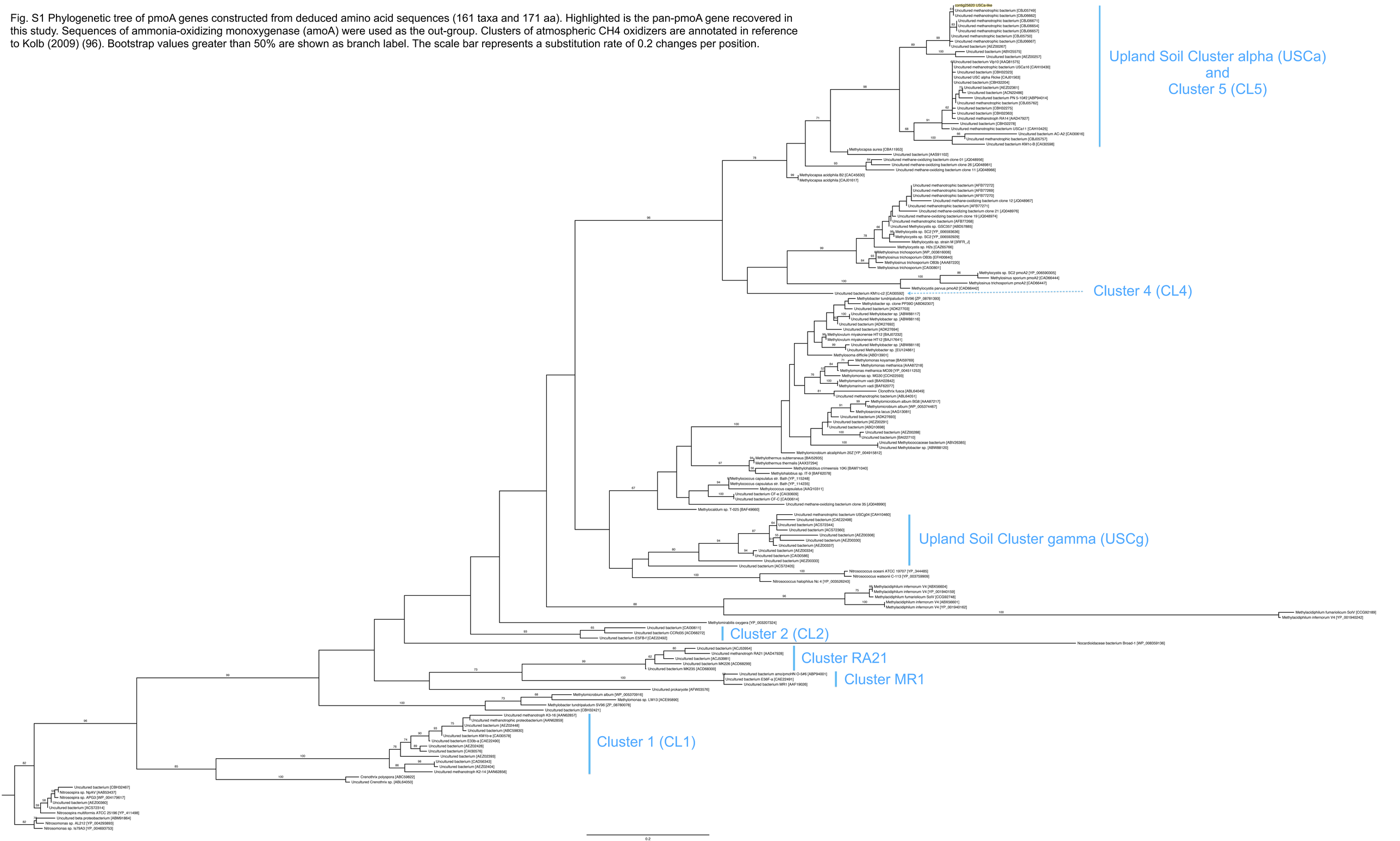

Fig. S2. Phylogenetic tree of pmoB genes constructed from deduced amino acid sequences (69 taxa and 377 aa). Highlighted are the pan-pmoB genes recovered in this study. Sequences of ammonia-oxidizing monoxygenase (amoB) were used as the out-group. Bootstrap values greater than 50% are shown as branch label. The scale bar represents a substitution rate of 0.2 changes per position.

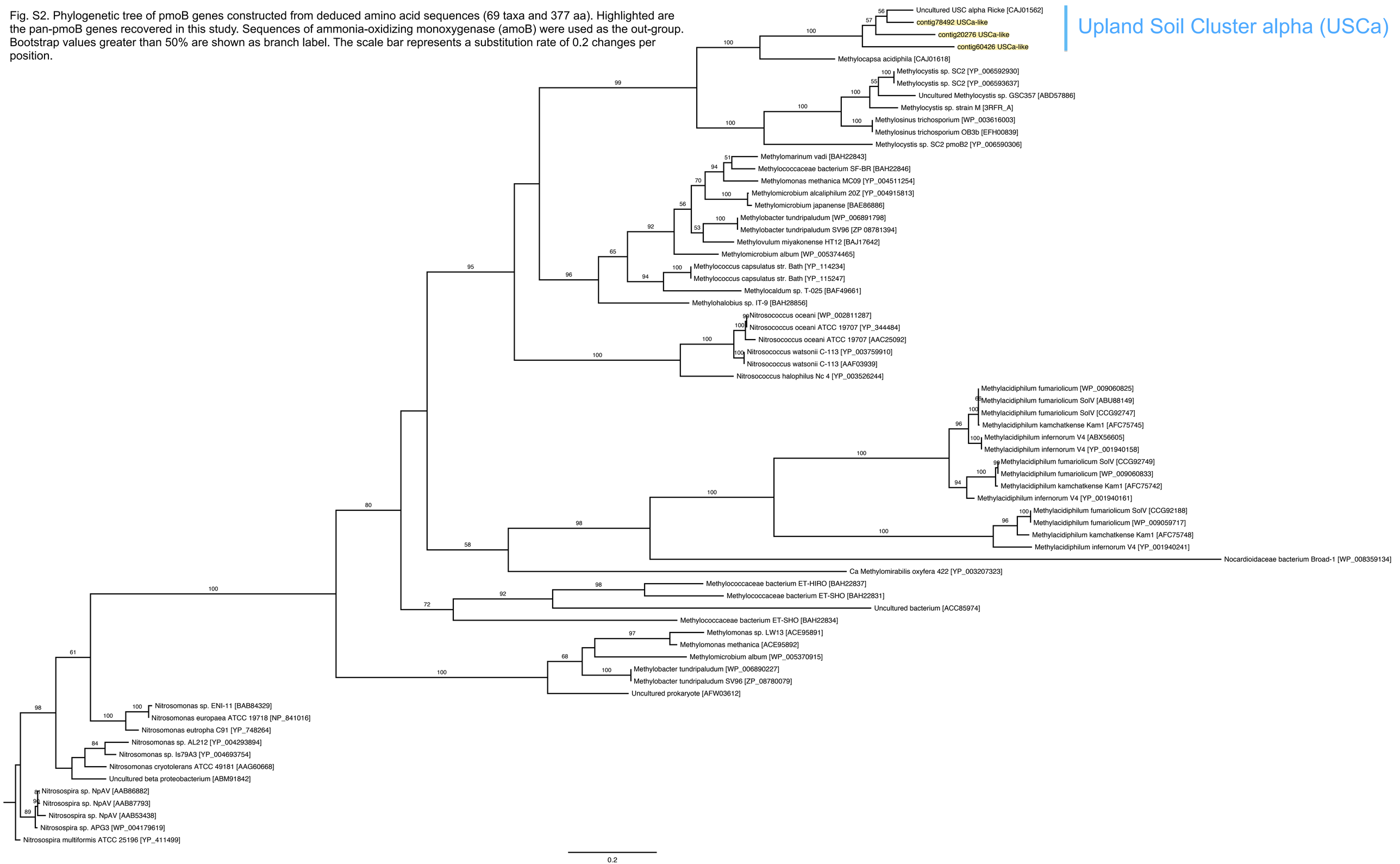

Fig. S3. Phylogenetic tree of pmoC genes constructed from deduced amino acid sequences (82 taxa and 244 aa). Highlighted are the pan-pmoC genes recovered in this study. Sequences of ammonia-oxidizing monoxygenase (amoC) were used as the out-group. Bootstrap values greater than 50% are shown as branch label. The scale bar represents a substitution rate of 0.2 changes per position.

Upland Soil Cluster alpha (USCa)

contig19544 USCa-like
Uncultured USC alpha Ricke [CAJ01564]
contig25961 USCa-like
Methylocapsa acidiphila [CAJ01616]
Methylocystis sp. SC2 pmoC2 [YP_006590304]
Methylocystis sp. SC2 [YP_006593635]
Methylocystis sp. SC2 [YP_006592928]
Methylocystis sp. SC2 [YP_006590954]
Methylocystis sp. SC2 [CAE47799]
Methylosinus trichosporium [WP_003612568]
Methylosinus trichosporium OB3b [EFH02634]
Methylocystis sp. SC2 [CCD32212]
Methylosinus trichosporium OB3b [EFH00841]
Methylosinus trichosporium [WP_003616009]
Uncultured Methylocystis sp. GSC357 [ABD57884]
Methylocystis sp. strain M [3RFR_C]
Methylocystis sp. SC2 [YP_006590829]
Nitrosococcus watsonii C-113 [YP_003759908]
Nitrosococcus oceani ATCC 19707 [YP_344486]
Nitrosococcus halophilus Nc 4 [YP_003526242]
Methylomicrobium japanense [BAE86884]
Methylomicrobium alcaliphilum 20Z [YP_004915811]
Methylomicrobium album [WP_005374468]
Methylovulum miyakonense HT12 [BAJ17640]
Methylobacter tundripaludum [WP_006891796]
Methylobacter tundripaludum SV96 [ZP_08781392]
Methylococcaceae bacterium SF-BR [BAH22844]
Methylomonas methanica MC09 [YP_004511252]
Methylomarinum vadi [BAH22841]
Methylococcus capsulatus str. Bath [YP_115249]
Methylococcus capsulatus str. Bath [YP_114236]
Methylococcus capsulatus str. Bath [AAB49820]
Methylococcus capsulatus str. Bath [AAD43965]
Methylococcus capsulatus str. Bath [YP_112829]
Methylohalobius sp. IT-9 [BAH28855]
Uncultured gamma proteobacterium [BAL55376]
Methylocaldum sp. T-025 [BAF49659]
Uncultured gamma proteobacterium [BAL55374]
Methylacidiphilum fumariolicum SolV [CCG92751]
Methylacidiphilum fumariolicum [WP_009060837]
Methylacidiphilum fumariolicum SolV [ABU88151]
Methylacidiphilum kamchatkense Kam1 [AFC75740]
Methylacidiphilum infernorum V4 [YP_001940163]
Methylacidiphilum infernorum V4 [YP_001940152]
Methylacidiphilum infernorum V4 [ABX56606]
Methylacidiphilum infernorum V4 [YP_001940160]
Methylacidiphilum kamchatkense Kam1 [AFC75743]
Methylacidiphilum fumariolicum SolV [CCG92190]
Methylacidiphilum fumariolicum [WP_009059720]
Methylacidiphilum kamchatkense Kam1 [AFC75746]
Methylacidiphilum infernorum V4 [YP_001940243]
Ca Methylomirabilis oxyfera [YP_003207216]
Ca Methylomirabilis oxyfera [YP_003207325]
Mycobacterium chubuense NBB4 [YP_006442845]
Mycobacterium rhodesiae NBB3 [YP_005000795]
Nocardioidaceae bacterium Broad-1 [WP_008359138]
Methylobacter tundripaludum [WP_006890228]
Methylobacter tundripaludum SV96 [ZP_08780080]
Methylomicrobium album [WP_005370914]
Methylomonas sp. LW13 [ADC34235]
Methylococcaceae bacterium ET-HIRO [BAH22835]
Methylococcaceae bacterium ET-SHO [BAH22829]
Methylococcaceae bacterium ET-HIRO [BAH22838]
Methylococcaceae bacterium ET-SHO [BAH22832]
Nitrosomonas sp. AL212 [YP_004295287]
Nitrosomonas sp. AL212 [YP_004295767]
Nitrosomonas sp. AL212 [YP_004293892]
Nitrosomonas sp. Is79A3 [YP_004693752]
Nitrosomonas sp. Is79A3 [YP_004694476]
Uncultured beta proteobacterium [ABM91791]
Nitrosospira sp. NpAV [AAC69319]
Nitrosospira sp. NpAV [AAB53436]
Nitrosospira sp. NpAV [AAB87791]
Nitrosospira multiformis ATCC 25196 [YP_410877]
Nitrosomonas europaea ATCC 19718 [NP_842074]
Nitrosomonas europaea ATCC 19718 [NP_841018]
Nitrosomonas sp. ENI-11 [BAB84327]
Nitrosomonas sp. TK794 [BAA92238]
Nitrosomonas eutropha C91 [YP_748266]
Nitrosomonas eutropha C91 [YP_747730]
Nitrosomonas europaea ATCC 19718 [NP_841452]
Nitrosospira multiformis ATCC 25196 [YP_413148]

0.2

Fig. S4 Alignment of translated amino acids of *pmo*B contigs from metagenomic and metatranscriptomic libraries. Histidine residues (H33, H137 and H139) that coordinates the di-copper center (aka the active site of pMMO) are highlighted in blue. GenBank sequences YP_115247 and CAJ01562 encode for pmoB of MOB *Methylococcus capsulatus* str. Bath and atmMOB USCα.

Fig. S5. Predicted monthly air temperatures at Axel Heiberg Island, Canada. Monthly air temperatures at AHI during 1990s and 2090s were simulated through the Climate Model Intercomparison Project (CMIP5). T: Monthly air temperatures in 2011 at Eureka, Ellesmere Island, Nunavut, Canada downloaded from Total Carbon Column Observing Network (TCCON)

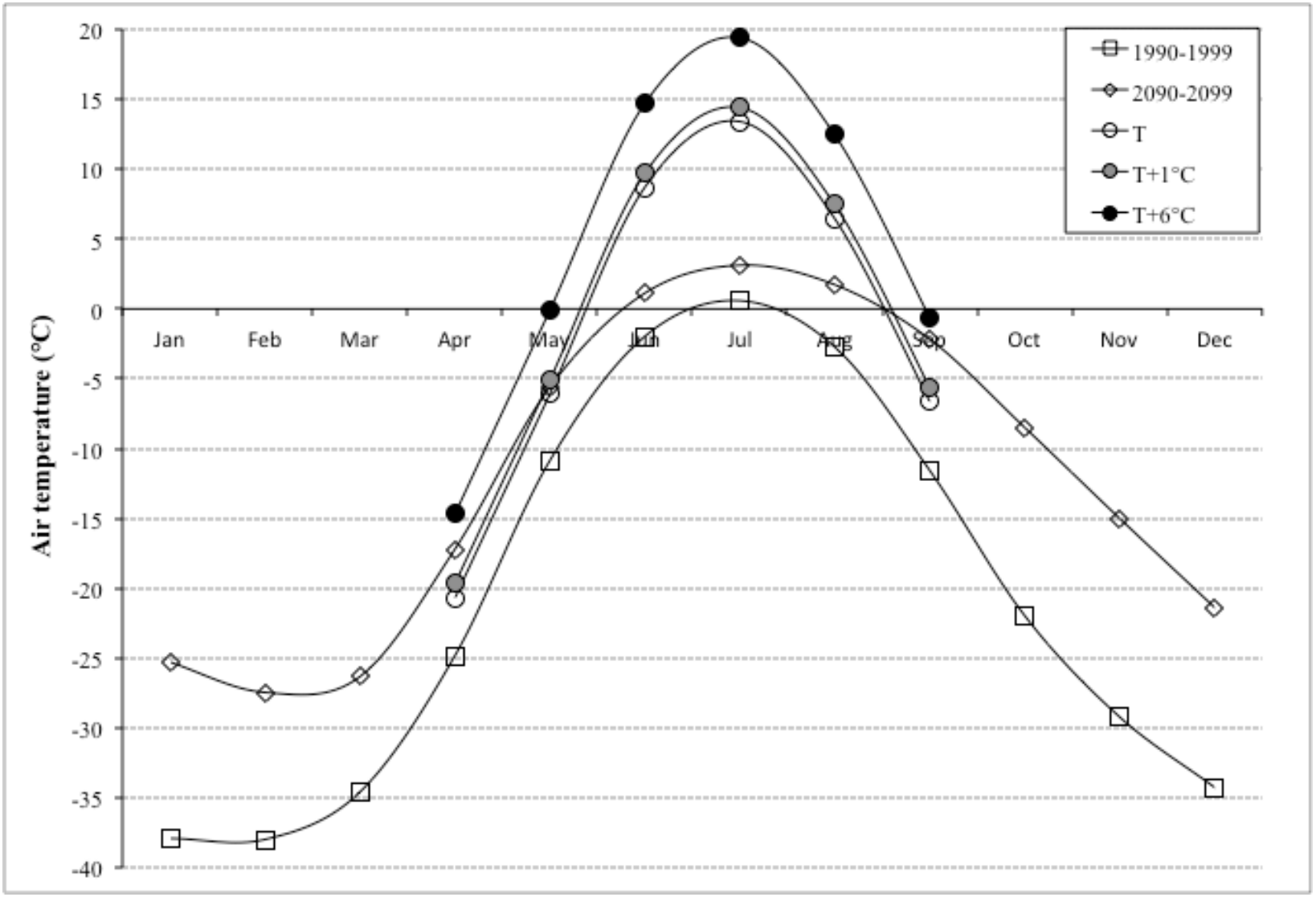

Table S1. CH_4 field fluxes in the Northern Circumpolar permafrost region.

CH_4 source

	Site	Latitude	Longitude	Soil description	Vegetation	pH	Soil moisture (wt%)	Bulk Soil C (wt%)	Field season	Soil temp. (°C)[1]	CH_4 flux (mg CH_4-C m^{-2} day^{-1})	Reference
1	Quttinirpaaq National Park, Ellesmere Island, Canada	82°47'60" N	71°24'00" W	Meadow wetland	Sedge/grass, moss meadow	NA	58.2±1.3 to 80.6±0.6	NA	2011 – 2012 late Jun – early Aug	8.2±0.1 to 10.8±0.2 @ 5 cm depth	0.12±0.11 to 0.32±0.33	Emmerton *et al.* (2014)
2	Ny-Ålesund, Svalbard	79° N	12° E	Arctic tundra	Cardamine	7 – 7.5	50 – 75	10 – 12	2008 Aug	NA	0.6	Adachi *et al.* (2006)
2	Ny-Ålesund, Svalbard	79° N	12° E	Arctic tundra	Salix	6 – 7.7	50 – 100	4 – 25	2008 Aug	NA	9.6	Adachi *et al.* (2006)
2	Ny-Ålesund, Svalbard	79° N	12° E	Arctic tundra	Oxyria/*Luzula*	6.5 – 7.5	40 – 50	4 – 10	2008 Aug	NA	2.4	Adachi *et al.* (2006)
2	Ny-Ålesund, Svalbard	79° N	12° E	Arctic tundra	Bryophyte	6.8 – 7.3	40 – 50	4 – 12	2008 Aug	NA	7.2	Adachi *et al.* (2006)
3	Alexandra Fjord, Ellesmere Island, Canada	78°53' N	75°55' W	Barren	Cryptogam, herb barren (Dolomitic)	7.6 – 7.8	31 – 46	0.41 – 0.52	2009 late Jun – early Aug	NA	0.4	Brummell *et al.* (2012)
3	Alexandra Fjord, Ellesmere Island, Canada	78°53' N	75°55' W	Mountain	Noncarbonate mountain complex (Granitic)	6.5 – 7.0	47 – 55	0.35 – 0.53	2009 late Jun and early Aug	NA	0.3	Brummell *et al.* (2012)
3	Alexandra Fjord, Ellesmere Island, Canada	78°53' N	75°55' W	Prostrate	Prostrate dwarf-shrub, herb tundra (Dryas)	5.5 – 6.9	58 – 79	0.35 – 1.54	2009 late Jun and early Aug	NA	0.2	Brummell *et al.* (2012)
3	Alexandra Fjord, Ellesmere Island, Canada	78°53' N	75°55' W	Arctic wetland	Sedge/grass, moss wetland (Wet sedge meadow)	6.4 – 6.6	75 – 92	0.05 – 6.85	2009 late Jun and early Aug	NA	37.7	Brummell *et al.* (2012)
4	Zackenberg Valley, Greenland	74°28' N	20°34' W	Arctic wetland - peat soil	Sedges (*Carex stans*, *Dupontia psilosantha* and *Eriophorum scheuchzeri*), mosses (*Tomenthypnum*, *Scorpidium*, *Aulacommium* and *Drepanocladus*)	6.9±0.2	92	NA	Jun 25 – Aug 2	6 to 11°C @ 10 cm depth	88.2 to 251.8	Ström *et al.* (2012)
4	Zackenberg Valley, Greenland	74°28' N	20°34' W	Arctic wetland - peat soil	Dryas, Cassiope, Salix and Eriophorum	5.1 – 5.4	40 – 100	3.8 – 15.4	NA	5.49±1.8 to 9.13±3.8°C @ 5 cm depth	NA	Elberling *et al.* (2004)
4	Rylekærene, Zackenberg Valley, Greenland	74°28' N	20°34' W	Arctic wetland - peat soil	Fens (*Eriophorum scheuchzeri*, *Carex stans*, *Dupontia psilosantha*, *Arctagrostis latifolia*, *E. triste*, *Alopecurus alpinus*, and *Salix arctica*), heaths (*Cassiope tetragona*, *Dyras octopetala* and *Vaccinium uliginosum*) and mosses (*Tomenthypnum*, *Scorpidium*, *Aulacommium* and *Drepanocladus*)	6.9±0.2	>100 below 3 cm (2008) and 10 cm (2009)	NA	2008 Jun 24 – 2009 Oct 31	0.5 to 10°C @ 10 cm depth	3.2 to 82.8	Tagesson *et al.* (2012)
4	Zackenberg Valley, Greenland	74°17'50" N	21°00'00" W	Arctic wetland - peat soil	*Eriophorum scheuchzeri*, *Dupontia psilosantha*, *Arctagrostis latifolia*	NA	NA	NA	2007 late Jun – early Oct	-4 to 12°C @ 5 cm depth	58.9	Mastepanov *et al.* (2008)
4	Zackenberg Valley, Greenland	74°17'50" N	21°00'00" W	Arctic wetland - peat soil	Hummocky fen (mosses, *Salix arctica* and *Polygonum viviparum*)	NA	NA	NA	2008 thaw season	15.5°C	7.6	Christensen *et al.* (2000)
4	Zackenberg Valley, Greenland	74°17'50" N	21°00'00" W	Arctic wetland - peat soil	Continuous fen (*Eriophorum scheuchzeri* and *Dupontia psilosantha*)	NA	NA	NA	2009 thaw season	14.9°C	4.4	Christensen *et al.* (2000)
4	Zackenberg Valley, Greenland	74°17'50" N	21°00'00" W	Arctic wetland - peat soil	Grassland (e.g. *Carex saxatilis*, *Eriophorum triste* and *Arctagrostis latifolia*)	NA	NA	NA	2010 thaw season	15.1°C	1.4	Christensen *et al.* (2000)
4	Zackenberg Valley, Greenland	74°17'50" N	21°00'00" W	Arctic wetland - peat soil	*Salix arctica* snowbeds (*Salix arctica*, Alopecurus alpinus *and* Pedicularis lapponica)	NA	NA	NA	2011 thaw season	13.7°C	8.8	Christensen *et al.* (2000)
5	Lena River Delta, Siberia	72°22'197" N	126°28'951" E	Submerged polygon	*Scorpidium* moss	7.1	100	NA	2009 early Jul	4 – 7°C	21.6	Liebner *et al.* (2011)
5	Lena River Delta, Siberia	72°22'13" N	126°29'10" E	Polygonal tundra	Vegetated	NA	NA	NA	2006 Jun – Sept	NA	14	Sachs *et al.* (2008)
5	Lena River Delta, Siberia	72°22'12" N	126°28'11" E	Wet polygonal tundra	*Carex aquatilis* (dominant vascular plant), mosses and lichens	NA	>100 below few cm at polygon centre and 35 cm at polygon rim	1.8 – 22.1	1999 Aug	1.6 to 6.7 °C @ 15 cm depth	3.2±0.6 to 21.0±4.1	Kutzbach *et al.* (2004)
6	Near Barrow, Alaska	71°18' N	156°35' W	Drained thaw-lake basin	Sedges	"acidic"	NA	76 – 84	NA	-10 to -18°C	NA	Bockheim (2007)
6	Near Barrow, Alaska	71°17'2.6" N	156°35'45.6" W	Wet meadow tundra	Vegetated	"acidic"	>100 below 2.5±5.2 cm	NA	2009 Aug – Oct	NA	22.8±2.5 (Eddy covariance) to 23.8±7.1 (Chamber)	Sturtevant *et al.* (2012)
6	Near Barrow, Alaska	71° N	156° W	Wet meadow tundra	Graminoids (incl. *Arctophila fulva*, *Dupontia fisheri*, *Eriophorum* spp., *Carex aquatilis*), mosses (incl. *Sphagnum*, *Dicranum elongatum*), lichens and a few prostrate dwarf shrubs (*Salix* spp., *Cassiope tetragona*)	NA	NA	NA	2011 Jun – Aug	3.3°C	4.5 to 96	Sturtevant & Oechel (2013)
7	Flakkerhuk, Disko Island, Greenland	69° N	53° W	Arctic wetland	Hummocks, willows (*Salix arctophila* and *Salid arctica*), herbaceous plants (*Pyrola grandiflora*), grasses (*Carex L.* and *Deschampsia alpina*), mosses (*Sphagnum*)	NA	~95 – 100	NA	2011 Jul 1-12	NA	3.05	Johansen *et al.* (2011)
7	Flakkerhuk, Disko Island, Greenland	69° N	53° W	Arctic wetland	Grasses (*Eriophorum vaginatum* and *Arctophila fulva*), mosses (*Sphagum*)	NA	~95 – 100	NA	2012 Jul 1-12	NA	2.30	Johansen *et al.* (2011)
8	Stordalen mire, Sweden	68°22' N	19°03' E	Intermediate thawed ground	*Sphagnum* spp. and *Carex* spp.	NA	NA	NA	2002 – 2007 (field measurements and gap-filling)	NA	8.6 to 21.1	Bäckstrand *et al.* (2010)
8	Stordalen mire, Sweden	68°22' N	19°03' E	Completely thawed ground	*Eriophorum angustifolium*	NA	NA	NA	2002 – 2007 (field measurements and gap-filling)	NA	66.5 to 101.5	Bäckstrand *et al.* (2010)
8	Stordalen mire, Sweden	68°21' N	18°49' E	Minerotrophic-sedge mire	*Eriophorum angustifolium* and *Sphagnum riparium* Angst.	5.4 – 6.0	>100 below 2 cm	24 – 59	2006 Jun, Aug and Sept	4.2 to 17.3°C @ 5 cm depth	NA	Lupascu *et al.* (2012)
8	Stordalen mire, Sweden	68°21' N	18°49' E	Minerotrophic-Sphagnum mire	*Sphagnum spp.*	4.1 – 4.4	>100 below 2 cm	~31 – 50	2007 Jun, Aug and Sept	3.4 to 13.7°C @ 5 cm depth	NA	Lupascu *et al.* (2012)
8	Stordalen mire, Sweden	68°21' N	18°49' E	Ombrotrophic bog	*Rubus chamaemorus* L., *Empetrum hermaphroditum* Hagerup., and *Andromeda polifolia* L.	4.0 – 4.2	20	~45	2008 Jun, Aug and Sept	3.5 to 13.2°C @ 5 cm depth	NA	Lupascu *et al.* (2012)
9	Hudson Bay lowlands	53° N	90° W	Boreal wetland		NA	NA	NA	NA	NA	40.8	Picket-Heaps *et al.* (2011)

CH_4 sink

	Site	Latitude	Longitude	Soil description	Vegetation	pH	Soil moisture (wt%)[1]	Bulk Soil C (wt%)	Field season	Soil temp. (°C)[1]	CH_4 flux (mg CH_4-C m^{-2} day^{-1})	Reference
a	Quttinirpaaq National Park, Ellesmere Island, Canada	82°47'60" N	71°24'00" W	Polar desert	Grass, prostrate dwarf-shrub forb tundra	7.2 – 7.3	9.4±0.1 to 17.5±0.2	1.4 – 1.48	2008 – 2012 late Jun – early Aug	11.1±0.4 to 13.7±0.3 @ 5 cm depth	-0.68±0.17 to -1.34±0.15	Emmerton *et al.* (2014)
a	Quttinirpaaq National Park, Ellesmere Island, Canada	82°47'60" N	71°24'00" W	Meadow wetland	Sedge/grass, moss meadow	NA	NA	NA	2011 – 2012 Jul (first 2 weeks)	NA	-0.30±0.09	Emmerton *et al.* (2014)
a	Patterson River, Ellesmere Island, Canada	82°35'47" N	63°45'32" W	Polar desert	Grass (<5% cover)	8.6 – 8.7	0.04 (Water-filled porosity)	5.18 – 7.17	2010 Jul 30 – Aug 1	1.4 to 4.4°C	-0.14±0.27 (Light) to -0.61±0.13 (Dark)	Brummell *et al.* (2014)
b	Expedition Fjord, Axel Heiberg Island, Canada	79°24'55" N	90°45'27" W	High-centered polygon	Lichen/mossess and sparse grass	NA	NA	NA	2011 Jul 15-16	12.3 to 18.4°C @ 5 cm depth	-0.11 to -0.17	Allan *et al.* (2014)
b	Expedition Fjord, Axel Heiberg Island, Canada	79°24'52" N	90°45'30" W	Arctic wetland	Cotton grass	NA	NA	NA	2011 Jul 15-16	7.9°C @ 5 cm depth	-0.13	Allan *et al.* (2014)
b	Expedition Fjord, Axel Heiberg Island, Canada	79°24'57" N	90°45'46" W	High-centered polygon	Sparse cover by grasses (e.g. *Puccinellia arctica*, *Salix arctica*, *Polygonum viviparum*, *Dryas* sp., *Saxifraga* sp., *Papaver* sp., *Eriophorum* sp.) and lichens	5.5 – 6	15 – 20	1 – 6	2011 Jul 9-14	12.4°C @ 5 cm depth	-0.07±0.01	Stackhouse *et al.* (submitted)
b	Expedition Fjord, Axel Heiberg Island, Canada	79°24'57" N	90°45'47" W	Ice wedge	Heavily cover by grasses (e.g. *Puccinellia arctica*, *Salix arctica*, *Polygonum viviparum*, *Dryas* sp., *Saxifraga* sp., *Papaver* sp., *Eriophorum* sp.)	5.5 – 6	15 – 20	1 – 6	2011 Jul 9-14	14.7°C @ 5 cm depth	-0.10±0.03	Stackhouse *et al.* (submitted)
b	Expedition Fjord, Axel Heiberg Island, Canada	79°24'57" N	90°45'46" W	High-centered polygon	Sparse cover by grasses (e.g. *Puccinellia arctica*, *Salix arctica*, *Polygonum viviparum*, *Dryas* sp., *Saxifraga* sp., *Papaver* sp., *Eriophorum* sp.) and lichens	5.5 – 6	15 – 20	1 – 6	2012 Jul 6-8	8.4°C @ 5 cm depth	-0.08±0.02	Stackhouse *et al.* (submitted)
b	Expedition Fjord, Axel Heiberg Island, Canada	79°24'57" N	90°45'46" W	High-centered polygon	Sparse cover by grasses (e.g. *Puccinellia arctica*, *Salix arctica*, *Polygonum viviparum*, *Dryas* sp., *Saxifraga* sp., *Papaver* sp., *Eriophorum* sp.) and lichens	5.5 – 6	15 – 20	1 – 6	2013 Jul 4-19	1.3 to 12.9°C @ 5 cm depth	-0.02±0.01 to -0.14±0.02	This study (using open-circuit method)
b	Expedition Fjord, Axel Heiberg Island, Canada	79°24'57" N	90°45'47" W	High-centered polygon	Sparse cover by grasses (e.g. *Puccinellia arctica*, *Salix arctica*, *Polygonum viviparum*, *Dryas* sp., *Saxifraga* sp., *Papaver* sp., *Eriophorum* sp.) and lichens	5.5 – 6	15 – 20	1 – 6	2013 mid Jul	9.2°C @ 5 cm depth	-0.84±0.18	This study (using closed-static method)
c	Ny-Ålesund, Svalbard	79° N	12° E	Arctic tundra	*Salix*	6 – 7.7	50 – 100	4 – 25	2008 Aug	NA	-2.4	Adachi *et al.* (2006)
c	Ny-Ålesund, Svalbard	79° N	12° E	Arctic tundra	*Oxyria*/*Luzula*	6.5 – 7.5	40 – 50	4 – 10	2008 Aug	NA	-3.6	Adachi *et al.* (2006)
c	Ny-Ålesund, Svalbard	79° N	12° E	Arctic tundra	Bryophyte	6.8 – 7.3	40 – 50	4 – 12	2008 Aug	NA	-4.8	Adachi *et al.* (2006)
d	Alexandra Fjord, Ellesmere Island, Canada	78°53' N	75°55' W	Hemiprostrate	Prostrate/hemiprostrate dwarf-shrub tundra (Cassiope)	6.3 – 7.0	54 – 75	0.26 – 0.52	2009 late Jun and early Aug	NA	-0.03	Brummell *et al.* (2012)
d	Alexandra Fjord, Ellesmere Island, Canada	78°53' N	75°55' W	Sedge/dwrafi-shrub	Nonmusock sedge, dwarf-shrub, moss tundra (Willow)	5.2 – 5.8	43 – 51	1.16 – 4.17	2009 late Jun and early Aug	NA	-0.1	Brummell *et al.* (2012)
d	Alexandra Fjord, Ellesmere Island, Canada	78°53' N	75°55' W	Arctic wetland	Sedge/grass, moss wetland (Wet sedge meadow)	6.4 – 6.6	75 – 92	0.05 – 6.85	2009 late Jun and early Aug	NA	-17.8	Brummell *et al.* (2012)
d	Dome, Ellesmere Island, Canada	78°51'31" N	75°55'37" W	Polar desert	Grass (<5% cover)	8.6	0.06 (Water-filled porosity)	3.61 – 4.78	2010 Jul 20-21	2.3 to 13.9°C	-1.55±0.32 (Dark) to -1.92±0.58 (Light)	Brummell *et al.* (2014)
e	Okse Bay, Ellesmere Island, Canada	77°8'88" N	87°39'10" W	Polar desert	Sedge/grass (<5% cover)	7.7 – 7.9	0.06 (Water-filled porosity)	3.32	2010 Jul 13-17	6.4 to 12.9°C	-1.15±0.31 (Dark) to -1.85±0.46 (Light)	Brummell *et al.* (2014)
f	Zackenberg Valley, Greenland	74°17'50" N	21°00'00" W	Arctic soil	*Cassiope* heaths (*Cassiope tetragona* and *Vaccinium uliginosum*)	NA	NA	NA	2007 thaw season	16.1°C	-0.02	Christensen *et al.* (2000)
f	Zackenberg Valley, Greenland	74°30' N	21°00' W	Arid lowland	Dwarf shrub (*Dryas octopetala* x *integrifolia*) and grasses (*Kobresia myosuroides*, *Carex rupestris* and *Poa glauca*)	7.25±0.04	~4 – 16	2 – 10	2009 Jul – Oct	-6.5 to 20°C @ 5 cm depth	NA	Christiansen *et al.* (2012)
g	Lena River Delta, Siberia	72°22'13" N	126°29'10" E	Submerged polygon	*Scorpidium* moss	7.1	100	NA	2009 early Jul	4 to 7°C	-1.7	Liebner *et al.* (2011)
h	Flakkerhuk, Disko Island, Greenland	69° N	53° W	Arctic tundra	Willows (*Salix arctica*, *Salix glauca*)	NA	~35 – 40	NA	2013 Jul 1-12	NA	-0.78	Johansen *et al.* (2011)
h	Flakkerhuk, Disko Island, Greenland	69° N	53° W	Arctic tundra	Willows (*Salix arctica*, *Salix glauca*), heaths (*Cassiope tetragona*), birches (*Betula nana*), shrubs (*Empetrum hermaphroditum*)	NA	~25	NA	2014 Jul 1-12	NA	-1.18	Johansen *et al.* (2011)
i	Stordalen mire, Sweden	68°22' N	19°03' E	Drained palsa areas	Woody herbaceous vegetation	NA	NA	NA	2002 – 2007 (field measurements and gap-filling)	-20 to 20°C[3]	<-9	Bäckstrand *et al.* (2010)
i	Stordalen mire, Sweden	68°22' N	19°03' E	Intermediate thawed ground	*Sphagnum* spp. and *Carex* spp.	NA	NA	NA	2002 – 2007 (field measurements and gap-filling)	-20 to 20°C[3]	<-11	Bäckstrand *et al.* (2010)
j	Bonanza Creek, Alaska, USA	64°45' N	148°18' W	Upland soils	North-facing black spruce	5	491	91	1990 Oct	0.2°C @ 10 cm depth	-0.41	Whalen *et al.* (1992)
j	Bonanza Creek, Alaska, USA	64°45' N	148°18' W	Upland soils	south-facing aspen (*Populus tremuloides*)	6.4	56	16	1990 Oct	3.6°C @ 10 cm depth	-0.17	Whalen *et al.* (1992)
j	Bonanza Creek, Alaska, USA	64°45' N	148°18' W	Upland soils	North-facing birch (*Betula papyrifera*)	5.9	69	24	1990 Oct	3.3°C @ 10 cm depth	-0.47	Whalen *et al.* (1992)
j	Bonanza Creek, Alaska, USA	64°45' N	148°18' W	Upland soils	South-facing white spruce (*Picea glauca*)	4.9	139	50	1990 Oct	2.2°C @ 10 cm depth	-0.41	Whalen *et al.* (1992)
k	Unalaska Island, Aleutian Islands	53° N	167° E	Moist tundra meadow	Mosses, liches, cottongrasses (*Eriophorum* sp.), low-lying ferns and dwarf shrubs (*Vaccinium* sp.)	NA	>100	16 – 38	1987 Oct	7°C	-2.03	Whalen & Reeburg (1990)

Note:
[1] Percentage by weight (wt%) unless specified
[2] Ambient temperature unless specified
[3] Temperature range in year 2004
NA: Not available

Table S2. Methanotrophic (A) and methanogenic (B) taxa identified in near-surface cryosols (at 5 cm depth) in the intact core warming experiments.

(A)

Class/Phylum	Family	Genus[1]	Dominant Species	Mean % abundance > 0.001% (± SD)[3]	Methanotrophy/Type of Intracytoplasmic membrane (ICM)	Formaldehyde Assimilation Pathway	Type of MMO[4]
α-Proteobacteria	Beijerinckiaceae	*Methylocapsa*	*Methylocapsa acidophila*[2]	0.0046 (±0.0024)	Facultative/Type II	Serine	pMMO only
α-Proteobacteria	Beijerinckiaceae	*Methylocella*	*Methylocella silvestris*	0.2930 (±0.1124)	Facultative/Type II	Serine	sMMO only
α-Proteobacteria	Methylocystaceae	*Methylocystis*	*Methylocystis* sp. ATCC 49242	0.0921 (±0.0282)	Obligate/Type II	Serine	pMMO & sMMO
α-Proteobacteria	Methylocystaceae	*Methylosinus*	*Methylosinus trichosporum*	0.0966 (±0.0309)	Obligate/Type II	Serine	pMMO & sMMO
				Subtotal = 0.49%			
γ-Proteobacteria	Methylococcaceae	*Methylobacter*	*Methylobacter tundripaludum*	0.0446 (±0.0118)	Obligate/Type I	Ribulose monophosphate (RuMP)	pMMO & sMMO
γ-Proteobacteria	Methylococcaceae	*Methylococcus*	*Methylococcus capsulatus*	0.0706 (±0.0191)	Obligate/Type I	Ribulose monophosphate (RuMP)	pMMO & sMMO
				Subtotal = 0.12%			
Verrucomicrobia	Methylacidiphilaceae	*Methylacidiphilum*	*Methylacidiphilum infernorum*	0.0887 (±0.0200)	Obligate/No ICM	Serine variant	pMMO only
				Total =0.69%			

(B)

Phylum	Class	Family	Genus[5]	Mean % abundance > 0.001% (± SD)[3]	Methanogenesis pathway
Euryarchaeota	Methanobacteria	Methanobacteriaceae	*Methanobrevibacter*	0.0011 (±0.0033)	Hydrogenotrophic
Euryarchaeota	Methanobacteria	Methanobacteriaceae	*Methanothermobacter*	0.0107 (±0.0080)	Hydrogenotrophic
Euryarchaeota	Methanobacteria	Methanothermaceae	*Methanothermus*	0.0011 (±0. 0018)	Hydrogenotrophic
Euryarchaeota	Methanococci	Methanocaldococcaceae	*Methanocaldococcus*	0.0052 (±0.0103)	Hydrogenotrophic
Euryarchaeota	Methanococci	Methanococcaceae	*Methanococcus*	0.0034 (±0.0054)	Hydrogenotrophic
Euryarchaeota	Methanococci	Methanocellaceae	*Methanocella*	0.0081 (±0.0065)	Hydrogenotrophic
Euryarchaeota	Methanococci	Methanocorpusculaceae	*Methanocorpusculum*	0.0010 (±0.0270)	Hydrogenotrophic
Euryarchaeota	Methanococci	Methanomicrobiaceae	*Methanoculleus*	0.0035 (±0.0100)	Hydrogenotrophic
Euryarchaeota	Methanococci	Methanospirillaceae	*Methanospirillum*	0.0085 (±0.0123)	Hydrogenotrophic
Euryarchaeota	Methanococci	Methanomicrobiales	*Methanoregula*	0.0163 (±0.0101)	Hydrogenotrophic
Euryarchaeota	Methanococci	Methanomicrobiales	*Methanosphaerula*	0.0120 (±0.0100)	Hydrogenotrophic
Euryarchaeota	Methanococci	Methanosaetaceae	*Methanosaeta*	0.0072 (±0.0071)	Aceticlastic
Euryarchaeota	Methanococci	Methanosarcinaceae	*Methanococcoides*	0.0088 (±0.0056)	Methylotrophic
Euryarchaeota	Methanococci	Methanosarcinaceae	*Methanohalobium*	0.0029(±0.0049)	Methylotrophic
Euryarchaeota	Methanococci	Methanosarcinaceae	*Methanohalophilus*	0.0027 (±0.0023)	Methylotrophic
Euryarchaeota	Methanococci	Methanosarcinaceae	*Methanosarcina*[6]	0.0686 (±0.0263)	Aceticlastic
				Total =0.16%	

Notes:

[1]Genera not detected: *Clonothrix*, *Crenothrix*, *Methylohalobius*, *Methylosoma*, *Methylothermus*, *Methylosphaera*, *Methylomarinum*, *Methylocaldum* and *Methylogaea*.

[2]The closest related isolate to atm CH_4-oxidizing bacterium Upland Soil Cluster alpha (USCα), as proposed by the phylogeny of the pmoCAB operon and 4 other open read frames (Ricke et al., 2005)

[3]Mean abundance of 16 cryosol samples collected at different time during the course of incubation (1 week, 6 and 12 months).

[4]MMO: Methane monooxygenase; pMMO: particulate MMO; sMMO: soluble MMO

[5]Genera that were sporadically present in some samples with a relative abundances < 0.001% include: *Methanobacterium*, *Methanosphaera*, *Methanothermus*, *Methanothermococcus*, *Methanoplanus* and *Methanopyrus*.

[6]This genus contains representatives that are capable of oxidizing CH_4 anaerobically.

Table S3. Genes of methane monooxygenases and homologous enzymes identified in (A) metagenome data from near-surface cryosols (at 5 cm depth) in the intact core warming experiments and (B) metatranscriptome data from the polygon trough sample (collected on July 15, 2013).

(A)

					Closest protein match (BlastX)				
De Novo Assembly ID[1]	**Size (bp)**	**Mean % abundance (± SD)[2]**	**Putative gene**		**Accesion no.**	**Taxon**	**Protein superfamily**	**Enzyme Encoded**	**% of identity**
Contig25620	1117	0.00015 (±0.00014)	*pmo*A		CAJ01563.1	Upland soil cluster alpha (USCalpha)	Pmo/Amo	α subunit of particulate methane monoxygenase (27-kDa)	87
Contig19544	1301	0.00015 (±0.00012)	*pmo*C		CAJ01564.1	Upland soil cluster alpha (USCalpha)	Pmo/Amo	γ subunit of particulate methane monoxygenase	85
Contig25961	1116	0.00029 (± 0.00033)	*pmo*A		CAJ01564.1	Upland soil cluster alpha (USCalpha)	Pmo/Amo	α subunit of particulate methane monoxygenase (27-kDa)	73
			*pmo*C		CAJ01565.1	Upland soil cluster alpha (USCalpha)	Pmo/Amo	γ subunit of particulate methane monoxygenase	86
Contig60426	646	0.00005 (± 0.00003)	*pmo*B		CAJ01562.1	Upland soil cluster alpha (USCalpha)	Pmo/Amo	β subunit of particulate methane monoxygense (45-kDa)	70
Contig78492	528	0.00003 (± 0.00003)	*pmo*B		CAJ01562.1	Upland soil cluster alpha (USCalpha)	Pmo/Amo	β subunit of particulate methane monoxygense (45-kDa)	85
Contig20276	1272	0.00013 (± 0.00009)	*pmo*B		CAJ01562.1	Upland soil cluster alpha (USCalpha)	Pmo/Amo	β subunit of particulate methane monoxygense (45-kDa)	84
			Unknown		CAJ01561.1	Upland soil cluster alpha (USCalpha)		Conserved hypothetical protein	74
Contig01417	4093	0.00039 (± 0.00033)	*amo*C		YP_006863929.1	Candidatus Nitrososphaera gargensis Ga9.2	Pmo/Amo	Subunit C of ammonia monooxygenase/methane monooxygenase	95
			*amo*A		AEQ03735.1	Uncultured crenarchaeote	Pmo/Amo	Subunit A of ammonium monooxygenase	99
Contig08394	1973	0.00011 (± 0.00009)	*pmo* homolog		YP_001239622.1	Bradyrhizobium sp. BTAi1	Ferritin-like	α subunit of methane/phenol/toluene monooxygenase	97
Contig62491	620	0.00006 (± 0.00002)	*pmo* homolog		YP_481616.1	Frankia sp. CcI3	Ferritin-like	Methane monooxygenase	83
Contig61701	655	0.00012 (± 0.00003)	*pmo* homolog		YP_004330745.1	Pseudonocardia dioxanivorans CB1190	Ferritin-like	Methane monooxygenase	96
Contig61059	630	0.00006 (± 0.00004)	*pmo* homolog		YP_005283808.1	Gordonia polyisoprenivorans VH2	Ferritin-like	Small subunit of putative phenol and propane monooxygenase	68
Contig46385	636	0.00006 (± 0.00003)	*pmo* homolog		WP_010242492.1	Pseudonocardia sp. P1	Ferritin-like	Methane monoxygenase	68
Contig56456	674	0.00005 (± 0.00003)	*pmo* homolog		WP_016880985.1	Rhodococcus sp. DK17	Ferritin-like	Methane monoxygenase	88

(B)

					Closest protein match (BlastX)				
De Novo Assembly ID[3]	**Size (bp)**	**Mean % abundance**	**Putative gene**	**Closest metagenome match (contig ID in Table S3a)**	**Accesion no.**	**Taxon**	**Protein superfamily**	**Enzyme Encoded**	**% of identity**
Contig_6812	288	0.00042%	*pmo*C	Contig25961	CAJ01564.1	Upland soil cluster alpha (USCalpha)	Pmo/Amo	γ subunit of particulate methane monoxygenase	90
Contig_7751	236	0.00011%	*pmo*C	Contig25961	CAJ01564.1	Upland soil cluster alpha (USCalpha)	Pmo/Amo	γ subunit of particulate methane monoxygenase	66
Contig_6846	284	0.00011%	*pmo*C	Contig19544	CAJ01564.1	Upland soil cluster alpha (USCalpha)	Pmo/Amo	γ subunit of particulate methane monoxygenase	90
Contig_6861	435	0.00007%	*pmo*A	Contig25620	CBJ05749.1	Upland soil cluster alpha (USCalpha)	Pmo/Amo	β subunit of particulate methane monoxygense (45-kDa)	98
Contig_7936	454	0.00005%	*pmo*B	-	CAJ01562.1	Upland soil cluster alpha (USCalpha)	Pmo/Amo	β subunit of particulate methane monoxygense (45-kDa)	88
Contig_7223	346	0.00008%	*pmo*B	Contig60426	CAJ01562.1	Upland soil cluster alpha (USCalpha)	Pmo/Amo	β subunit of particulate methane monoxygense (45-kDa)	84
Contig_7286	344	0.00005%	*pmo*B	Contig20276	CAJ01562.1	Upland soil cluster alpha (USCalpha)	Pmo/Amo	β subunit of particulate methane monoxygense (45-kDa)	83
Contig_5304	570	0.00018%	*amo*C	Contig01417	YP_006863092.1	Candidatus Nitrososphaera gargensis Ga9.2	Pmo/Amo	Subunit C of ammonia monooxygenase/methane monooxygenase	97
Contig_2448	491	0.00015%	*pmo* homolog	Contig56456	WP_018330673.1	Actinomycetospora chiangmaiensis	Ferritin-like	Methane monooxygenase	90
Contig_6461	411	0.00020%	*pmo* homolog	Contig62491	YP_004330745.1	Pseudonocardia dioxanivorans CB1190	Ferritin-like	Methane monooxygenase	94

Notes:
[1]Metagenome contigs are available on MG-RAST (ID: 4530050.3)
[2]Mean abundance of 10 cryosol samples collected at different time during the course of incubation (T=1 week and 6 months).
[3]Metatranscriptome (or transcript) contigs are available on MG-RAST (ID: 4548477.3)

Table S4. Aerobic methanotrophs detected in Arctic permafrost-affected region

				Martineau *et al.* (2010)	Martineau *et al.* (2010)	Yergeau *et al.* (2010)	Yergeau *et al.* (2010)	Wilhelm *et al.* (2011)	Martineau *et al.* (2014)	Martineau *et al.* (2014)	Martineau *et al.* (2014)	This study	This study	Wartiainen *et al.* (2003)	Tveit *et al.* (2012)	Tveit *et al.* (2012)	Graef *et al.* (2011)	Liebner *et al.* (2009)	Liebner *et al.* (2009)	Wagner *et al.* (2005)	Liebner *et al.* (2007)	Barbier *et al.* (2012)	Liebner *et al.* (2013)	Mackelprang *et al.* (2011)	Kaliuzhnaia *et al.* (2002)	Pacheco-Oliver *et al.* (2002)	Pacheco-Oliver *et al.* (2002)	Pacheco-Oliver *et al.* (2002)
			Location	Eureka, Ellesmere Island, Canadian high Arctic	Eureka, Ellesmere Island, Canadian high Arctic	Eureka, Ellesmere Island, Canadian high Arctic	Eureka, Ellesmere Island, Canadian high Arctic	Expedition Fjord, Axel Heiberg Island, Canadian high Arctic	Expedition Fjord, Axel Heiberg Island, Canadian high Arctic	Expedition Fjord, Axel Heiberg Island, Canadian high Arctic	Expedition Fjord, Axel Heiberg Island, Canadian high Arctic	Expedition Fjord, Axel Heiberg Island, Canadian high Arctic	Expedition Fjord, Axel Heiberg Island, Canadian high Arctic	Spitsbergen, Svalbard, Norway	Ny – Ålesund, Svalbard, Norway	Ny – Ålesund, Svalbard, Norway	Spitsbergen, Svalbard, Norway	Smoylov Island, the Lena Delta, Siberia	Smoylov Island, the Lena Delta, Siberia	Samoylov Island, the Lena Delta, Siberia	Samoylov Island, the Lena Delta, Siberia	Drained Lake', Herschel Island, Candaian Arctic	Norway	Hess Creek, Alaska, US	Russia	Kuujjuaq, Northern Quebec, Canada	Kuujjuaq, Northern Quebec, Canada	Kuujjuaq, Northern Quebec, Canada
			Lat, Long	80.000N, 85.839W	80.000N, 85.839W	80.000N, 85.839W	80.000N, 85.839W	79.433N, 90.766W	79.433N, 90.766W	79.433N, 90.766W	79.433N, 90.766W	79.415N, 90.757W	79.415N, 90.757W	78.933N, 11.883E and 78.250N, 15.5000E	78.926N, 11.944E and 78.933N, 11.818E	78.926N, 11.944E and 78.933N, 11.818E	78.917N, 11.933E	72.367N, 126.467E	72.367N, 126.467E	72.367N, 126.467E	72.367N, 126.467E	69.729N, 138.957W	69.694N, 29.383E	65.670N, 149.077W	NA	NA	NA	NA
			Soil description	Wet tundra	Wet tundra	Tundra	Tundra	Wetland	Acidic	Upland tundra	Wet meadow	High-centered polygon	High-centered polygon	Wetland	Peat bog	Peat bog	Wetland	Rim of low-centered polygon	Rim of low-centered polygon	Rim of low-centered polygon	Rim of low-centered polygon	Low-centered polygon	Degrading palsa	Peat soil	Subarctic tundra	Peat-like tundra (K3)	Peat-like tundra (K3)	Peat-like tundra (K3)
			Vegetation cover	NA	NA	NA	NA	NA	NA	NA	NA	Vegetated	Vegetated	Vegetated	Vegetated	Vegetated	Vegetated	NA	NA	Vegetated	NA	Vegetated	Vegetated	Vegetated	NA	NA	NA	NA
			Depth below surface (cm)	0 – 10	0 – 10	Surface	Surface	14 – 19	0 – 15	0 – 15	0 – 15	0 – 5	0 – 5	0 – 10	0 – 10	0 – 10	0 – 6	41436	41436	0 – 20	0 – 18	0 – 20	0 – 10	Active layer	41409	15 – 30	15 – 30	15 – 30
			Soil pH	6.7 – 7.1	6.7 – 7.1	7.9	7.9	4.48	4.8	6.4	6	5.5	5.5	5.0 – 6.7	5.2 – 5.8	5.2 – 5.8	NA	6.5	6.5	7.9	NA	5.2 – 5.6	4.2	6.48	NA	8.35	8.35	8.35
			Soil water content (wt%)	16 – 23	16 – 23	12.7	12.7	29.6	NA	NA	NA	15 – 20	15 – 20	75 – 90	70 – 90	70 – 90	NA	NA	NA	26.2 – 30.1	15.7 – 26.2	77 – 79	NA	82	NA	14.1	14.1	14.1
			Soil organic content (wt%)	3.80 – 5.60	3.80 – 5.60	3	3	0.98	NA	NA	NA	1 – 6	1 – 6	24 – 87	90 – 91	90 – 91	NA	2.1	2.1	2.1 – 2.4	2.1 – 3	23 – 28	NA	40	NA	9.43	9.43	9.43
			Incubation condition of soil being studied (if applicable)	incubated soils at 4°C and RT in NMS medium with >8,000 ppmv CH_4	incubated soils at 4°C and RT in NMS medium with >8,000 ppmv CH_4	NA	NA	NA	Incubated soils at 10°C 10 and 1000 ppmv CH_4	Incubated soils at 10°C 10 and 1000 ppmv CH_4	Incubated soils at 10°C 10 and 1000 ppmv CH_4	Incubated at 4°C with 2 ppmv CH4 for 1 – 26 weeks	Incubated at 4°C with 2 ppmv CH4 for 1 – 26 weeks	NA	NA	NA	Incubated at 15C with 10,000 and 50,000 ppmv of $^{13}CH_4$	NA	NA	NA	NA	NA	NA	Incubated soils at 5°C for 1 week with 20 ppmv CH_4 (trapped in frozen soils)	NA	NA	NA	NA
			Molecular method^	PCR-DGGE	PCR-DGGE	Meta-genomics	qPCR	PCR-DGGE	PCR-Cloning and Microarray	PCR-Cloning and Microarray	PCR-Cloning and Microarray	Meta-genomics	Meta-genomics	PCR-DGGE	Meta-transcriptomics	Meta-transcriptomics	PCR-Cloning	PCR-DGGE	PCR-DGGE	GC/MS	FISH	PCR-Cloning and TRFLP	PCR-Cloning	PCR	PCR	PCR-Cloning	PCR-Cloning	PCR-Cloning
			Biomarker	16S rDNA (universal)	pmoA	all genes (but no pmoA)	16S rDNA (methanotroph-specific)	16S rDNA (universal)	pmoA	pmoA	pmoA/ amoA	pmo	All raw sequences	16S rDNA (methanotroph-specific)	16S rRNA	pmoA	16S rRNA (universal)	16S rDNA (methanotroph-specific)	pmoA	PFLA	16S rDNA (methanotroph-specific)	pmoA	pmoA (no transcripts and no mmoX)	16S rDNA (methanotroph-specific)	16S rDNA (methanotroph-specific)	pmoA	mmoX	16S rRNA (methanotroph-specific)
Phylum	**Class**	**Family**	**Genus**																									
Proteobacteria																												
	Alpha-proteobacteria						x		x		x																	
		Beijerinckiaceae																			x			X				
			Methylocapsa										x									x							
			Methylocella										X																
			Methyloferula																										
		Methylocystaceae																											
			Methylocystis					X					x									x			x			x	
			Methylosinus										x	x						x		X	X						
			Methylosinus trichosporium																	x		x							
		Upper soil cluster alpha							X	x	x	X															X	x	
	Gamma-proteobacteria						X																						
		Methylococcaceae				X													X		X			x				
			Clonothrix																			x							
			Crenothrix																										
			Methylobacter		x				x	x																			
			Methylobacter luteus	x																			x		x				
			Methylobacter psychrophilus											x	x														
			Methylobacter tundripaludum	x	X								x	X	X	X		X											
			Methylocaldum														X						x						
			Methylococcus										x																
			Methylogaea																										
			Methylohalobius						x	x	x																		
			Methylomarinum																										
			Methylomicrobium																										
			Methylomonas																	x					x				
			Methylosarcina																	x					x				
			Methylosoma												x					x									
			Methylosphaera																										
			Methylothermus																	x					x				
			Methylovulum																										
		Upper soil cluster gamma								X																			
Uncharacterized pmoA/amoA										x	X																		
Verrucomicrobia																													
	Verrucomicrobiae																												
		Methylacidiphilaceae																											
			Methylacidiphilum										x																

Notes:
Beige highlighted cells are soil samples with empirical support of atmospheric CH_4 oxidation
Blue highlighted species are known pschrophilic or psychrotolerant methanotrophs
"X" and "x" indicate the presence of methanotrophs in the sample and "X" denotes the most dominant group. For studies that the relative abundance of methanotrophs is not known, "x" informs only the taxa being detected (no implication on the dominance).
Columns to the right of the dotted lines are studies of sub-Arctic regions which are provided as reference
NA: Not available

Table S5. Methanotrophic proteins identified in near-surface cryosols (at 5 cm depth) in the intact core warming experiments.

Sample	Locus[1]	Sequence Count	Spectrum Count	Sequence Coverage	Protein Length	Adjusted NSAF[2]	Descriptive Name	MolWt (Daltons)	pI	XCorr	DeltCN	ObsM+H+	CalcM+H+	Ion%	Peptide Count	Sequence[3]	Charge
Core A15, 1wk thaw (Techical replicate 1)	pMMOJGIMGRASTw1Acontig00008*	2	2	34.7%	75	22.8	pmoB [unculturedbacterium]	7873	5.2	4.54	0.76	1613.8099	1614.7526	70.0%	1	R.GLSLSDNSPIAPGETR.D	2
	pMMOw1w26Acontig00005*	2	2	34.7%	75	22.8	pmoB [unculturedbacterium]	7873	5.2	2.60	0.51	1086.4727	1088.2059	61.1%	1	R.DVAVTIQDAR.W	2
	fig|543016.3.peg.43*	2	2	10.9%	247	6.9	[Methylocapsa USClike uncultured] [Particulate methane monooxygenase B-subunit (EC 1.14.13.25)]	27489	9.6	3.51	0.72	1840.9594	1842.0563	65.6%	1	R.NIQALENEVDSGPITIK.Y	2
	pmoB_contig00023*	2	2	6.5%	413	4.1	manually translated USCalphalikepMMO	45464	7.1	3.22	0.64	1077.5647	1078.2133	94.4%	1	R.IGEFNTAGLR.F	2
Core A15, 1wk thaw (Technical replicate 2)	fig|543016.3.peg.43*	3	6	15.4%	247	224.9	[Methylocapsa USClike uncultured] [Particulate methane monooxygenase B-subunit (EC 1.14.13.25)]	27489	9.6	3.29	0.79	1840.9528	1842.0563	62.5%	1	R.NIQALENEVDSGPITIK.Y	2
	pmoB_contig00023*	3	6	9.2%	413	134.5	manually translated USCalphalikepMMO	45464	7.1	3.20	0.58	1077.5667	1078.2133	94.4%	3	R.IGEFNTAGLR.F	2
										2.72	0.67	1353.668	1354.5022	90.0%	2	K.VEYPDYLLADR.G	2
	gi|83308654|emb|CAJ01562.1|	2	4	4.7%	427	86.7	pmoB [Uncultured USCa Ricke]	47044	8.5	3.20	0.58	1077.5667	1078.2133	94.4%	3	R.IGEFNTAGLR.F	2
										2.66	0.52	1073.5527	1074.179	83.30%	1	R.DVAVTVQDAR.W	2
Core A15, 1wk thaw (Technical replicate 3)	pMMOJGIMGRASTw1Acontig00008*	2	3	21.3%	75	65.5	pmoB [unculturedbacterium]	7873	5.2	4.28	0.75	1613.8127	1614.7526	63.3%	2	R.GLSLSDNSPIAPGETR.D	2
	pMMOw1w26Acontig00005*	2	3	21.3%	75	65.5	pmoB [unculturedbacterium]	7873	5.2	1.80	0.70	1617.13	1614.7526	30.0%	1	R.GLSLSDNSPIAPGETR.D	1
	fig|543016.3.peg.43*	4	6	15.4%	247	39.8	[Methylocapsa USClike uncultured] [Particulate methane monooxygenase B-subunit (EC 1.14.13.25)]	27489	9.6	3.06	0.75	1840.9568	1842.0563	62.5%	1	R.NIQALENEVDSGPITIK.Y	2
										2.66	0.52	1077.5645	1078.2133	72.2%	3	R.IGEFNTAGLR.F	2
	pmoB_contig00023*	4	6	9.2%	413	23.8	manually translated USCalphalikepMMO	45464	7.1	1.99	0.52	1077.57	1078.2133	44.4%	1	R.IGEFNTAGLR.F	1
										2.57	0.57	1353.6667	1354.5022	85.0%	1	K.VEYPDYLLADR.G	2
	gi|83308654|emb|CAJ01562.1|	2	4	2.3%	427	15.3	pmoB [Uncultured USCa Ricke]	47044	8.5	2.66	0.52	1077.5645	1078.2133	72.2%	3	R.IGEFNTAGLR.F	2
										1.99	0.52	1077.57	1078.2133	44.4%	1	R.IGEFNTAGLR.F	1
Core A7, 12 month thaw (Technical replicate 1)	fig|543016.3.peg.43*	2	4	8.5%	247	18.3	[Methylocapsa USClike uncultured] [Particulate methane monooxygenase B-subunit (EC 1.14.13.25)]	27489	9.6	3.26	0.69	1077.5636	1078.2133	94.4%	3	R.IGEFNTAGLR.F	2
	pmoB_contig00023*	2	4	5.1%	413	10.9	manually translated USCalphalikepMMO	45464	7.1	2.67	0.64	1353.6624	1354.5022	80.0%	1	K.VEYPDYLLADR.G	2
	gi|83308654|emb|CAJ01562.1|	2	4	4.7%	427	10.6	pmoB [Uncultured USCa Ricke]	47044	8.5	3.26	0.69	1077.5636	1078.2133	94.4%	3	R.IGEFNTAGLR.F	2

Notes:
[1]Contig sequences generated by our studies are marked with an asterisk.
[2]NSAF: Normalized Spectral abundance factor. Adjusted NSAF values are NSAF values multiplied by 1000000.
[3]Unique peptide sequences are highlighted using the same colour scheme as in Fig. 2.